



HAL
open science

Local transparent boundary conditions for wave propagation in fractal trees (I). Method and numerical implementation

Patrick Joly, Maryna Kachanovska

► **To cite this version:**

Patrick Joly, Maryna Kachanovska. Local transparent boundary conditions for wave propagation in fractal trees (I). Method and numerical implementation. SIAM Journal on Scientific Computing, 2021, 10.1137/20M1362334 . hal-02462264v3

HAL Id: hal-02462264

<https://hal.science/hal-02462264v3>

Submitted on 3 Aug 2020

HAL is a multi-disciplinary open access archive for the deposit and dissemination of scientific research documents, whether they are published or not. The documents may come from teaching and research institutions in France or abroad, or from public or private research centers.

L'archive ouverte pluridisciplinaire **HAL**, est destinée au dépôt et à la diffusion de documents scientifiques de niveau recherche, publiés ou non, émanant des établissements d'enseignement et de recherche français ou étrangers, des laboratoires publics ou privés.

LOCAL TRANSPARENT BOUNDARY CONDITIONS FOR WAVE PROPAGATION IN FRACTAL TREES (I). METHOD AND NUMERICAL IMPLEMENTATION

PATRICK JOLY * AND MARYNA KACHANOVSKA *

Abstract. This work is dedicated to the construction and analysis of high-order transparent boundary conditions for the weighted wave equation on a fractal tree, which models sound propagation inside human lungs. This article follows the works [9, 6], aimed at the analysis and numerical treatment of the model, as well as the construction of low-order and exact discrete boundary conditions. The method suggested in the present work is based on the truncation of the meromorphic series that represents the symbol of the Dirichlet-to-Neumann operator, in the spirit of the absorbing boundary conditions of B. Engquist and A. Majda. We analyze its stability and convergence, as well as present computational aspects of the method. Numerical results confirm theoretical findings.

Key words. Wave equation, fractal, metric graph, Dirichlet-to-Neumann operator

AMS subject classifications. 35L05, 65M12, 34B45

1. Introduction. Modelling sound propagation in a human lung is important for medical diagnostics, see e.g. the Audible Human Project [1], [17] and references therein. Because the physical phenomenon of wave propagation in a lung is highly complex and multi-scale, its computational tractability relies on the use of simplified models. One of such models is based on the geometric representation of a bronchiolar tree as a self-similar network of tubes, see [15, 5, 16]. An asymptotic analysis of the 3D wave equation posed on such a network, with respect to the thickness of the tubes tending to zero, leads to a weighed 1D wave equation on a self-similar infinite tree, see [10, 18]. This model is somewhat non-standard, and its mathematical analysis was performed in [9], which gave rise to many ideas of the present paper.

Because such a tree has infinitely many edges, to perform any kind of numerical simulations, we need to be able to truncate the computational domain. This is classically done via introducing 'absorbing' boundary conditions, which, in turn, are based on an approximation of the Dirichlet-to-Neumann (DtN) operator. The principal difficulty lies in its time non-locality. One of the methods for approximating the DtN, based on the convolution quadrature [12, 13], was proposed in [6]. Since the cost of this method is quadratic in the number of time steps, in this work we suggest an alternative method to approximate the DtN, which follows the classical ideas of Engquist and Majda [4], namely, approximation of its symbol by rational fractions.

Compared to the classical case of free space wave propagation, there are multiple additional difficulties associated to the model we study. In particular, it describes wave propagation in highly heterogeneous media, and exhibits multi-scale phenomena. As a result, no closed form expression for the Green function is available. Nonetheless, in [9] it was shown that the symbol of the DtN operator is a meromorphic function, which satisfies a certain non-linear equation. This symbol can be represented as a convergent series of rational functions with simple real poles. To approximate the symbol of the DtN, we truncate this series at several first poles that are closest to the origin. This approximation leads to high-order approximated transparent boundary conditions and can be realized via local operators in the time domain. We prove the stability of such boundary conditions and perform the error analysis; moreover, we

*POEMS, UMR 7231 CNRS-ENSTA-INRIA, Institut Polytechnique de Paris, Palaiseau, France (patrick.joly@inria.fr, maryna.kachanovska@inria.fr).

demonstrate how to choose the number of poles to achieve a desired accuracy.

This article is organized as follows. Section 2 introduces the notations and the problem. Section 3 contains the description, stability and convergence analysis of the method. Section 4 deals with the error control and the complexity of the method. In Section 5 we present numerical aspects of the method and numerical results. Finally, Section 6 is dedicated to conclusions and open problems.

Let us mention that this article is companion of [8], where we develop a quantitative error analysis for the approximate high-order transparent boundary conditions introduced in the the present work.

2. Problem setting. This section is not new, and presents a shortened version of the corresponding section in [6]. The definitions can be found as well in [9].

2.1. Notation. Given $p \in \mathbb{N}_*$, let \mathcal{T} be a p -adic tree (a collection of vertices and edges), which satisfies:

- \mathcal{T} is rooted, i.e. there exists a vertex M^* designated as a 'root' of the tree;
- the root vertex M^* is incident to a single edge (the 'root edge') of the tree;
- every edge of the tree has p children edges (p -adicity); this in particular implies that the tree has infinitely many vertices and edges.

For such a tree we can introduce a notion of a generation. A generation \mathcal{G}^n is a set of edges that is defined inductively in the following way: \mathcal{G}^0 contains a root edge only; \mathcal{G}^{n+1} contains all children edges of the edges from \mathcal{G}^n . The p^n edges belonging to \mathcal{G}^n will be denoted by $\Sigma_{n,k}$, $k = 0, \dots, p^n - 1$. The edge $\Sigma_{n,k}$ has p children

$$(2.1) \quad \Sigma_{n+1,pk+j}, \quad j = 0, \dots, p-1.$$

By \mathcal{T}^m we denote the subtree of \mathcal{T} containing the first $m+1$ generations, i.e. $\bigcup_{\ell=0}^m \mathcal{G}^\ell$.

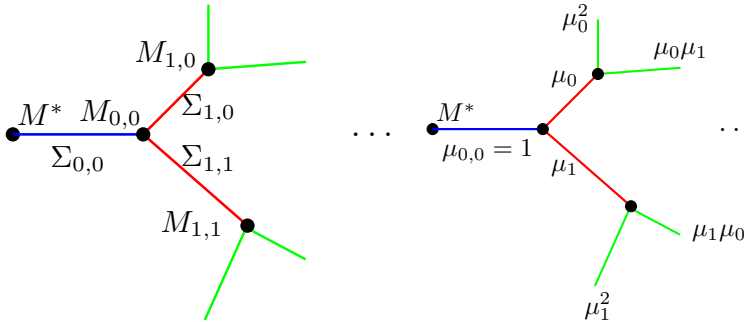


FIGURE 1. *Left: A self-similar p -adic ($p = 2$) infinite tree. In blue we mark the edges that belong to \mathcal{G}^0 , in red the edges of \mathcal{G}^1 , in green the edges of \mathcal{G}^2 . Right: Distribution of weights on the edges of a 2-adic infinite self-similar tree.*

We will study metric trees, i.e. trees in which edges are identified with segments on the real line. Thus, to each of the edges $\Sigma_{n,k}$ one can assign a length $\ell_{n,k} > 0$. This allows to define a notion of a distance $d(M, M^*)$ between the given vertex M and the root vertex M^* as a sum of lengths of the edges that connect M to M^* .

To define a notation for the vertices, similar to $\Sigma_{n,k}$ for edges, let us consider an edge $\Sigma_{n,k}$. Provided that it is incident to two vertices M_0, M_1 , let us set $M_{n,k} :=$

$\operatorname{argmax}_{V \in \{M_0, M_1\}} d(V, M^*)$. This notation allows to identify all the vertices in a unique manner; a respective illustration is provided in Figure 1, left.

Besides its length $\ell_{n,k}$, with every edge $\Sigma_{n,k}$ we associate another quantity, namely a weight $\mu_{n,k} > 0$ (see also Remark 2.3). W.l.o.g., we assume that $\mu_{0,0} = 1$.

In what follows, we will consider self-similar (fractal) trees, see [9, Definition 2.3]. To define them, let $\boldsymbol{\alpha} := (\alpha_0, \dots, \alpha_{p-1}) \in (\mathbb{R}_*^+)^p$ and $\boldsymbol{\mu} := (\mu_0, \dots, \mu_{p-1}) \in (\mathbb{R}_*^+)^p$. Then the length/weight of the edge $\Sigma_{n+1,pk+j}$ (see 2.1) is related to the length/weight of its parent edge $\Sigma_{n,k}$ according to the following law:

$$\ell_{n+1,pk+j} = \alpha_j \ell_{n,k}, \quad \mu_{n+1,pk+j} = \mu_j \mu_{n,k}, \quad j = 0, \dots, p-1.$$

This is illustrated in Figure 1, right.

We will call a reference tree the tree, for which the length of its root edge $\ell_{0,0}$ is equal to 1. Unless stated otherwise, we will always assume that \mathcal{T} is a reference tree. Additionally, we will assume that $|\boldsymbol{\alpha}|_\infty := \max_j \alpha_j < 1$.

REMARK 2.1. *This assumption implies that with some $C > 0$, $d(M_{n,j}, M^*) < C$ for all $n \in \mathbb{N}$, $j = 0, \dots, p^n - 1$.*

REMARK 2.2. *When $p = 1$, \mathcal{T} can be identified with a bounded interval on \mathbb{R} .*

REMARK 2.3. *We refer to [11, 18] for the physical meaning of the weights $\mu_{n,k}$ in an asymptotic modelling of the human lung. The simplified model of a human lung that we consider has the following parameters: $p = 2$ and for all i , $\alpha_i \approx \alpha = 0.84$, see [20, p.125] and $\mu_i = \mu \approx 0.8$, see [20, p.123] and the asymptotic analysis in [11, 18].*

2.2. The weighted wave equation on a fractal tree. In order to introduce the model under consideration, we define a parameterization of an edge $\Sigma_{n,j}$ by an abscissa $s \in [0, \ell_{n,j}]$. The parametrization is introduced so that $\ell_{n,j}$ is associated to the vertex $M_{n,j}$. We additionally introduce a measure on $\Sigma_{n,j}$ as a usual Lebesgue measure on the interval $[0, \ell_{n,j}]$.

Let s be an abscissa on the tree \mathcal{T} (for each edge $\Sigma_{n,j}$ defined as above); formally, let us define the weight function μ on \mathcal{T} as follows: $\mu(s) = \mu_{n,j}$, $s \in \Sigma_{n,j}$ (with an obvious abuse of notation). We look for an acoustic pressure $u : \mathcal{T} \times \mathbb{R}^+ \rightarrow \mathbb{R}$. On each edge, u satisfies the wave equation with a source term: $u_{n,j} = u|_{\Sigma_{n,j}}$ solves

$$(2.2) \quad \partial_t^2 u_{n,j} - \partial_s^2 u_{n,j} = f_{n,j} \quad \text{on } \Sigma_{n,j}, \quad j = 0, \dots, p^n - 1, \quad n \geq 0,$$

$$(2.3) \quad u(M^*, t) = 0, \quad u(\cdot, 0) = \partial_t u(\cdot, 0) = 0.$$

The above introduces an infinite system of PDEs; they are coupled through the following continuity (\mathcal{C}) and Kirchoff (\mathcal{K}) conditions at all the vertices, see (2.1) (with an obvious abuse of notation)

$$(\mathcal{C}) \quad u_{n,j}(M_{n,j}, t) = u_{n+1,pj+k}(M_{n,j}, t), \quad k = 0, \dots, p-1,$$

$$(\mathcal{K}) \quad \partial_s u_{n,j}(M_{n,j}, t) = \sum_{k=0}^{p-1} \mu_k \partial_s u_{n+1,pj+k}(M_{n,j}, t), \quad j = 0, \dots, p^n - 1, \quad n \geq 0.$$

This problem needs to be equipped with the boundary conditions, obviously, at the root vertex M^* of the tree, as done in (2.3), but also at the 'infinite' boundary of the tree. This becomes clearer if one recalls that when $p = 1$, the tree \mathcal{T} can be identified to an interval on the real line, cf. Remark 2.2. If, additionally, $\mu_0 = 1$, the problem (2.2, 2.3, \mathcal{C} , \mathcal{K}) reduces to the IVP for the wave equation on an interval, whose well-posedness necessitates defining boundary conditions at both ends of the interval. This will be done in the weak form, by using a proper Sobolev space framework.

2.3. Dirichlet and Neumann BVPs for (2.2, 2.3, \mathcal{C} , \mathcal{K}).

2.3.1. Sobolev Spaces.

For a function $v : \mathcal{T} \rightarrow \mathbb{R}$, let

$$(2.4) \quad \int_{\mathcal{T}} \mu v := \sum_{n=0}^{\infty} \sum_{k=0}^{p^n-1} \int_{\Sigma_{n,k}} \mu_{n,k} v(s) ds$$

Let $C(\mathcal{T})$ be a space of continuous functions on \mathcal{T} , and

$$C_0(\mathcal{T}) := \{v \in C(\mathcal{T}) : v = 0 \text{ on } \mathcal{T} \setminus \mathcal{T}^m, \text{ for some } m \in \mathbb{N}\}.$$

Next, we introduce the following three Hilbert spaces of functions on \mathcal{T} . First of all,

$$L_{\mu}^2(\mathcal{T}) = \{v : v|_{\Sigma_{n,j}} \in L^2(\Sigma_{n,j}), \|v\|_{L_{\mu}^2(\mathcal{T})} < \infty\}, \quad \|v\|^2 = \|v\|_{L_{\mu}^2(\mathcal{T})}^2 = \int_{\mathcal{T}} \mu |v|^2.$$

We will denote by (\cdot, \cdot) the associated scalar product. Next, the weighted Sobolev space H_{μ}^1 is defined in a natural way:

$$H_{\mu}^1(\mathcal{T}) := \{v \in C(\mathcal{T}) \cap L_{\mu}^2(\mathcal{T}) : \|\partial_s v\| < \infty\}, \quad \|v\|_{H_{\mu}^1(\mathcal{T})}^2 = \|v\|^2 + \|\partial_s v\|^2.$$

Similarly, we define the corresponding spaces $L_{\mu}^2(\mathcal{T}^m)$ and $H_{\mu}^1(\mathcal{T}^m)$ on a truncated tree \mathcal{T}^m . The associated L_{μ}^2 -scalar product will be denoted by $(\cdot, \cdot)_{\mathcal{T}^m}$, and the norm by $\|\cdot\|_{\mathcal{T}^m}$. The remaining space, by analogy with H_0^1 , is defined as the closure:

$$H_{\mu,0}^1(\mathcal{T}) := \overline{C_0(\mathcal{T}) \cap H_{\mu}^1(\mathcal{T})}^{\|\cdot\|_{H_{\mu}^1(\mathcal{T})}}.$$

REMARK 2.4. *We work with real-valued function spaces, and indicate explicitly where complex-valued function spaces (and complex scalar products) are used.*

2.3.2. The BVP problems. First of all, let us introduce the two additional spaces (for brevity denoted in what follows by $V_{\mathbf{n}}$, $V_{\mathbf{d}}$):

$$V_{\mathbf{n}}(\mathcal{T}) = \{v \in H_{\mu}^1(\mathcal{T}) : v(M^*) = 0\}, \quad V_{\mathbf{d}}(\mathcal{T}) = \{v \in H_{\mu,0}^1(\mathcal{T}) : v(M^*) = 0\}.$$

These spaces differ from $H_{\mu}^1(\mathcal{T})$ (resp. from $H_{\mu,0}^1(\mathcal{T})$) by the condition at M^* .

As discussed in the end of Section 2.2, let us define the Neumann and Dirichlet problems for (2.2, 2.3, \mathcal{C} , \mathcal{K}), with 'Neumann' ('Dirichlet') referring to the conditions at the fractal boundary of the tree.

DEFINITION 2.5 (Time-domain Neumann problem). *Find*

$$(N) \quad \begin{aligned} u_{\mathbf{n}} &\in C(\mathbb{R}^+; V_{\mathbf{n}}) \cap C^1(\mathbb{R}^+; L_{\mu}^2(\mathcal{T})), \text{ s.t. } u_{\mathbf{n}}(\cdot, 0) = \partial_t u_{\mathbf{n}}(\cdot, 0) = 0, \text{ and} \\ &(\partial_t^2 u_{\mathbf{n}}, v) + (\partial_s u_{\mathbf{n}}, \partial_s v) = (f, v), \quad \text{for all } v \in V_{\mathbf{n}}. \end{aligned}$$

DEFINITION 2.6 (Time-domain Dirichlet problem). *Find*

$$(D) \quad \begin{aligned} u_{\mathbf{d}} &\in C(\mathbb{R}^+; V_{\mathbf{d}}) \cap C^1(\mathbb{R}^+; L_{\mu}^2(\mathcal{T})), \text{ s.t. } u_{\mathbf{d}}(\cdot, 0) = \partial_t u_{\mathbf{d}}(\cdot, 0) = 0, \text{ and} \\ &(\partial_t^2 u_{\mathbf{d}}, v) + (\partial_s u_{\mathbf{d}}, \partial_s v) = (f, v), \quad \text{for all } v \in V_{\mathbf{d}}. \end{aligned}$$

It is easy to see that the above problems imply (2.2, 2.3, \mathcal{C} , \mathcal{K}); they are well-posed if $f \in L^1_{loc}(\mathbb{R}^+; L^2_\mu(\mathcal{T}))$, cf. [6, Theorem 1]. It appears that in some cases the solutions to (N) and (D) coincide. To explain this result in more detail, let us introduce

$$\langle \mu \alpha \rangle := \sum_{i=0}^{p-1} \mu_i \alpha_i, \quad \left\langle \frac{\mu}{\alpha} \right\rangle \equiv \langle \mu / \alpha \rangle := \sum_{i=0}^{p-1} \frac{\mu_i}{\alpha_i}.$$

With the above definitions, we have

THEOREM 2.7. [9] *If $\langle \mu \alpha \rangle \geq 1$ or $\langle \mu / \alpha \rangle \leq 1$, the spaces $H^1_{\mu,0}(\mathcal{T})$ and $H^1_\mu(\mathcal{T})$ coincide, and thus $u_n = u_\partial$. Otherwise, $H^1_{\mu,0}(\mathcal{T}) \subsetneq H^1_\mu(\mathcal{T})$, and $u_n \neq u_\partial$.*

2.4. Transparent boundary conditions. Because the tree \mathcal{T} is structurally infinite, in order to perform the numerical simulations, it is necessary to truncate the tree to a finite number of generations. However, imposing simple Dirichlet or Neumann boundary conditions at the boundary of the truncated tree \mathcal{T}^m does not allow to reach a reasonable accuracy unless m is sufficiently large, cf. [9]. Because the computational costs increase exponentially with m (since at the m -th level there are p^m branches of the tree), this leads to a significant computational overhead. The main goal of this section is the definition of transparent BCs, which allow to perform accurate simulations on trees \mathcal{T}^m with m arbitrary small.

Our construction is based on the results of [9] (see also [6]). In what follows, we fix $m \geq 1$. We will assume that

ASSUMPTION 2.8. *The source term $f(\cdot, t)$ is supported in \mathcal{T}^{m-1} for all $t \geq 0$.*

2.4.1. Notations. We denote by $\Gamma_m := \{M_{m,j} : j = 0, \dots, p^m - 1\} \equiv \mathbb{R}^{p^m}$ the 'outer' boundary of \mathcal{T}^m .

Let $\mathbf{V}_\mu(\mathcal{T}^m) := \{v \in H^1_\mu(\mathcal{T}^m) : v(M^*) = 0\}$. For $v \in \mathbf{V}_\mu(\mathcal{T}^m)$, we define its trace:

$$(2.5) \quad \gamma_m : \mathbf{V}_\mu(\mathcal{T}^m) \rightarrow \mathbb{R}^{p^m}, \quad \gamma_m v = (v(M_{m,0}), \dots, v(M_{m,p^m-1})).$$

Let us additionally introduce, for $v \in \mathbf{V}_\mu(\mathcal{T}^m)$, $f_1, f_2 : \mathbb{R} \rightarrow \mathbb{R}$, $\mathbf{h} \in \mathbb{R}^{p^m}$,

$$(2.6) \quad \int_{\Gamma_m} f_1(\mu) f_2(\alpha) \mathbf{h} \gamma_m v := \sum_{j=0}^{p^m-1} f_1(\mu_{m,j}) f_2(\alpha_{m,j}) h_j v(M_{m,j}).$$

2.4.2. Transparent boundary conditions: definition. Our goal is to compute the restriction of the solution u_a to the tree \mathcal{T}^m . This means that we need to solve (2.2, 2.3, \mathcal{C} , \mathcal{K}) for $n = 0, \dots, m$, equipped with certain boundary conditions at Γ_m . These boundary conditions should be chosen so that the exact solution u_a satisfy them (hence the name 'transparent'). We will express them using DtN operators:

$$(2.7) \quad -\mu_{m,j} \partial_s u_{m,j}(M_{m,j}, t) = \mathcal{B}_{m,j}^a(\partial_t) u_{m,j}(M_{m,j}, t), \quad j = 0, \dots, p^m - 1,$$

where $\mathcal{B}_{m,j}^a(\partial_t)$, $\mathbf{a} \in \{\partial, \mathbf{n}\}$, is the exact DtN operator associated to the point $M_{m,j}$ (see Remark 2.9 for an explanation of the notation $\mathcal{B}_{m,j}^a(\partial_t)$). To clarify the meaning of $\mathcal{B}_{m,j}^a(\partial_t)$, let us introduce the following space:

$$H^1_{0,loc}(\mathbb{R}^+) := \{v \in H^1_{loc}(\mathbb{R}^+) : v(0) = 0\}.$$

Then $\mathcal{B}_{m,j}^a(\partial_t) \in \mathcal{L}(H^1_{0,loc}(\mathbb{R}^+), L^2_{loc}(\mathbb{R}^+))$, cf. [7]. To define its action, let us first fix $g \in H^1_{0,loc}(\mathbb{R}^+)$. Let $\mathcal{T}_k := \mathcal{T}_{m+1, pj+k}$, $k = 0, \dots, p-1$, be a p -adic self-similar infinite

subtree of \mathcal{T} , whose root vertex is $M_{m,j}$ and the root edge is $\Sigma_{m+1,pj+k}$, cf. (2.1). Then the DtN operator is defined as:

$$(2.8) \quad \mathcal{B}_{m,j}^{\mathbf{a}}(\partial_t)g = - \sum_{k=0}^{p-1} \mu_{m,j} \mu_k \partial_s u_{g,k}^{\mathbf{a}}(M_{m,j}, \cdot),$$

where $u_{g,k}^{\mathbf{a}} \in C^1(\mathbb{R}^+; \mathbf{L}_{\mu}^2(\mathcal{T}_k))$ satisfies:

1. if $\mathbf{a} = \mathfrak{d}$, $u_{g,k}^{\mathfrak{d}} \in C(\mathbb{R}^+; \mathbf{H}_{\mu,0}^1(\mathcal{T}_k))$ solves the Dirichlet problem:

$$(2.9) \quad \begin{aligned} (\partial_t^2 u_{g,k}^{\mathfrak{d}}, v)_{\mathcal{T}_k} + (\partial_s u_{g,k}^{\mathfrak{d}}, \partial_s v)_{\mathcal{T}_k} &= 0, \quad \text{for all } v \in V_{\mathfrak{d}}(\mathcal{T}_k), \\ u_{g,k}^{\mathfrak{d}}(M_{m,j}, t) &= g(t), \quad u_{g,k}^{\mathfrak{d}}(\cdot, 0) = \partial_t u_{g,k}^{\mathfrak{d}}(\cdot, 0) = 0. \end{aligned}$$

2. if $\mathbf{a} = \mathfrak{n}$, $u_{g,k}^{\mathfrak{n}} \in C(\mathbb{R}^+; \mathbf{H}_{\mu}^1(\mathcal{T}_k))$ solves (2.9) with $V_{\mathfrak{d}}$ replaced by $V_{\mathfrak{n}}$.

Next, we show that all the operators $\mathcal{B}_{m,j}^{\mathbf{a}}(\partial_t)$ can be expressed with the help of a single operator $\Lambda_{\mathbf{a}}(\partial_t)$, which is the DtN map in the root vertex of the reference tree.

2.4.3. Reference DtN operator. Provided $g \in H_{0,loc}^1(\mathbb{R}^+)$, let us define the reference DtN operator on the reference tree \mathcal{T} (i.e. $\ell_{0,0} = 1$) as follows:

$$\Lambda_{\mathbf{a}}(\partial_t)g(t) = -\partial_s u_g^{\mathbf{a}}(M^*, t), \quad \text{where}$$

1. if $\mathbf{a} = \mathfrak{d}$, the function $u_g^{\mathfrak{d}} \in C(\mathbb{R}^+; \mathbf{H}_{\mu,0}^1(\mathcal{T})) \cap C^1(\mathbb{R}^+; \mathbf{L}_{\mu}^2(\mathcal{T}))$ solves

$$(2.10) \quad \begin{aligned} (\partial_t^2 u_g^{\mathfrak{d}}, v) + (\partial_s u_g^{\mathfrak{d}}, \partial_s v) &= 0, \quad \text{for all } v \in V_{\mathfrak{d}}, \\ u_g^{\mathfrak{d}}(M^*, t) &= g(t), \quad u_g^{\mathfrak{d}}(\cdot, 0) = \partial_t u_g^{\mathfrak{d}}(\cdot, 0) = 0. \end{aligned}$$

2. if $\mathbf{a} = \mathfrak{n}$, $u_g^{\mathfrak{n}} \in C(\mathbb{R}^+; \mathbf{H}_{\mu}^1(\mathcal{T})) \cap C^1(\mathbb{R}^+; \mathbf{L}_{\mu}^2(\mathcal{T}))$ solves (2.10) where $V_{\mathfrak{d}}$ is substituted by $V_{\mathfrak{n}}$.

As the coefficients of (2.10) are independent of time, $\Lambda_{\mathbf{a}}(\partial_t)$ is a convolution operator.

REMARK 2.9. *The notations $\Lambda_{\mathbf{a}}(\partial_t)$, $\mathcal{B}_{m,j}^{\mathbf{a}}(\partial_t)$ are adapted from the convolution quadrature theory, cf. [14], and indicate that the respective operators are convolution operators. A convolution operator $\mathcal{K}(\partial_t)$ is defined as (where the integral below is understood in the sense of a convolution of causal tempered distributions)*

$$(\mathcal{K}(\partial_t)g)(t) = \int_0^t k(t-\tau)g(\tau)d\tau, \quad g: \mathbb{R}^+ \rightarrow \mathbb{R}.$$

The Fourier-Laplace transform of its convolution kernel, namely

$$(2.11) \quad \mathcal{K}(\omega) = \mathcal{F}k := \int_0^{\infty} e^{i\omega t} k(t)dt, \quad \omega \in \mathbb{C}^+ = \{z \in \mathbb{C} : \text{Im } z \geq 0\},$$

is called the symbol of the operator $\mathcal{K}(\partial_t)$. We will use the boldface to distinguish between the operators and their symbols. Moreover, given $\gamma > 0$, we will use the notation $\mathcal{K}(\gamma\partial_t)$ for a convolution operator with a symbol $\mathcal{K}(\gamma\omega)$.

2.4.4. Transparent BCs via the reference DtN. According to [9], the operator $\mathcal{B}_{m,j}^{\mathbf{a}}(\partial_t)$ can be expressed as follows:

$$(2.12) \quad \mathcal{B}_{m,j}^{\mathbf{a}}(\partial_t) = \mu_{m,j} \alpha_{m,j}^{-1} \sum_{k=0}^{p-1} \frac{\mu_k}{\alpha_k} \Lambda_{\mathbf{a}}(\alpha_k \alpha_{m,j} \partial_t).$$

The above follows from the Kirchoff conditions (\mathcal{K}) and a scaling argument (recall that $\alpha_{m,j}$ is the length of the edge $\Sigma_{m,j}$). The expression (2.12) indicates that approximating $\mathcal{B}_{m,j}^{\mathbf{a}}(\partial_t)$ relies on approximating $\Lambda_{\mathbf{a}}(\partial_t)$.

2.4.5. The problem posed on the truncated tree \mathcal{T}^m . As explained in the beginning of Section 2.4, to compute numerically the solution to (D) (or (N)), we will use the transparent boundary conditions, constructed in the previous section. Consistently with the notation (2.5), let us introduce

$$(2.13) \quad \mathcal{B}_m^{\mathbf{a}}(\partial_t) = \text{diag}(\mathcal{B}_{m,0}^{\mathbf{a}}(\partial_t), \dots, \mathcal{B}_{m,p^m-1}^{\mathbf{a}}(\partial_t)).$$

After integration by parts applied to (D) (resp. (N)), the variational formulation with the transparent BCs reads: with $\mathbf{a} \in \{\mathfrak{d}, \mathfrak{n}\}$,

$$\text{find } u_m^{\mathbf{a}} \in C(\mathbb{R}^+; \mathbf{V}_{\mu}(\mathcal{T}^m)) \cap C^1(\mathbb{R}^+; L_{\mu}^2(\mathcal{T}^m)),$$

s.t. $u_m^{\mathbf{a}}(\cdot, 0) = \partial_t u_m^{\mathbf{a}}(\cdot, 0) = 0$ and, for all $v \in \mathbf{V}_{\mu}(\mathcal{T}^m)$,

$$(2.14) \quad (\partial_t^2 u_m^{\mathbf{a}}, v)_{\mathcal{T}^m} + (\partial_s u_m^{\mathbf{a}}, \partial_s v)_{\mathcal{T}^m} + \int_{\Gamma_m} \mathcal{B}_m^{\mathbf{a}}(\partial_t) \gamma_m u_m^{\mathbf{a}} \gamma_m v = (f, v)_{\mathcal{T}^m}.$$

In [6] it was proven that this problem is well-posed and that $u_m^{\mathbf{a}} = u_{\mathbf{a}}|_{\mathcal{T}^m}$.

THEOREM 2.10 (Theorem 2.6 in [6]). *For all $f \in L_{loc}^1(\mathbb{R}^+; L_{\mu}^2(\mathcal{T}))$ that satisfies Assumption 2.8, the problem (2.14) has a unique solution which is the restriction of the solution $u_{\mathbf{a}}$, $\mathbf{a} = \mathfrak{d}$ (resp. $\mathbf{a} = \mathfrak{n}$) to (D) (resp. (N)) to \mathcal{T}^m .*

3. Approximation of the transparent boundary conditions. As shown in Section 2.4.4, with (2.12) the question of approximating $\mathcal{B}_m^{\mathbf{a}}(\partial_t)$ can be reduced to the question of approximating $\Lambda_{\mathbf{a}}(\partial_t)$. However, the associated convolution kernel is not known neither in the time nor in the frequency domain. This section is dedicated to a design of a tractable approximation of the reference DtN. It is organized as follows: in Section 3.1 we provide an approximation of $\Lambda_{\mathbf{a}}(\partial_t)$ and analyze its error. Section 3.2 deals with the stability analysis of the respective coupled formulation, and Section 3.3 is dedicated to the error analysis.

3.1. Principal idea: truncated reference DtN operator.

3.1.1. Some preliminaries. The main idea of our approach relies on a representation of the symbol of the DtN as a meromorphic series. Let us provide more details on this. Given a non-negative Hermitian sesquilinear form

$$(3.1) \quad a(u, v) := \sum_{n=0}^{\infty} \sum_{k=0}^{p^n-1} \int_{\Sigma_{n,k}} \mu_{n,k} \partial_s u \partial_s \bar{v} ds,$$

let us define the following operators (where we work with complex-valued functions):

$$(3.2) \quad \mathcal{A}_\mathbf{a} : D(\mathcal{A}_\mathbf{a}) \rightarrow L_\mu^2(\mathcal{T}), \quad (\mathcal{A}_\mathbf{a}u, v) = a(u, v),$$

$$(3.3) \quad D(\mathcal{A}_\mathbf{a}) = \{v \in V_\mathbf{a} : \exists C(v) \geq 0, \text{ s.t. } |a(v, g)| < C(v)\|g\|_{L_\mu^2(\mathcal{T})}, \text{ for all } g \in V_\mathbf{a}\}.$$

In a strong form, $\mathcal{A}_\mathbf{a}$ can be recast into the operator $\mu^{-1}(s)\partial_s(\mu(s)\partial_s \cdot)$ on $L_\mu^2(\mathcal{T})$, with the Dirichlet boundary condition at M^* and the Neumann ($\mathbf{a} = \mathbf{n}$) or Dirichlet ($\mathbf{a} = \mathbf{d}$) boundary conditions at the fractal boundary of the tree \mathcal{T} .

In [9] the following result was shown (the condition $|\alpha|_\infty < 1$, see Remark 2.1, is necessary for its validity, see [18] for a counter-example when $|\alpha|_\infty \geq 1$).

THEOREM 3.1 ([9]). *The embedding of $H_\mu^1(\mathcal{T})$ into $L_\mu^2(\mathcal{T})$ is compact.*

Therefore, the resolvent of $\mathcal{A}_\mathbf{a}$ is compact, thus the spectrum of $\mathcal{A}_\mathbf{a}$ is a pure point spectrum. We define its eigenvalues and normalized eigenfunctions as

$$(3.4) \quad \mathcal{A}_\mathbf{a}\varphi_{\mathbf{a},n} = \omega_{\mathbf{a},n}^2\varphi_{\mathbf{a},n}, \quad \|\varphi_{\mathbf{a},n}\|_{L_\mu^2(\mathcal{T})} = 1, \quad 0 < \omega_{\mathbf{a},1}^2 \leq \omega_{\mathbf{a},2}^2 \leq \dots \rightarrow +\infty,$$

The eigenvalues do not vanish, as shown in [9, Remark 1.20]. Using a spectral representation of the operator $\mathcal{A}_\mathbf{a}$ it is possible to show the following result.

THEOREM 3.2 (Proposition 1.23, discussion after (144) in [9]). *The symbol of the reference DtN operator $\Lambda_\mathbf{a}$, $\mathbf{a} \in \{\mathbf{n}, \mathbf{d}\}$, satisfies*

$$(3.5) \quad \Lambda_\mathbf{a}(\omega) = \Lambda_\mathbf{a}(0) - \sum_{n=1}^{+\infty} \frac{a_{\mathbf{a},n}\omega^2}{(\omega_{\mathbf{a},n})^2 - \omega^2}, \quad a_{\mathbf{a},n} = \omega_{\mathbf{a},n}^{-2} (\partial_s \varphi_{\mathbf{a},n}(M^*))^2.$$

The above series converges uniformly on compact subsets of $\mathbb{C} \setminus \{\pm\omega_{\mathbf{a},n}, n \in \mathbb{N}_\}$.*

Surprisingly, the values of $\Lambda_\mathbf{a}(0)$ will play an important role in the error analysis.

PROPOSITION 3.3 (Lemma 5.5, Corollary 5.6 in [9]). *$\Lambda_\mathbf{a}(0)$ is given by*

- if $\langle \mu/\alpha \rangle \leq 1$, then $\Lambda_\mathbf{d} \equiv \Lambda_\mathbf{n}$ and $\Lambda_\mathbf{d}(0) = 0$.
- if $\langle \mu\alpha \rangle < 1 < \langle \mu/\alpha \rangle$, then $\Lambda_\mathbf{d}(0) = 1 - \langle \mu/\alpha \rangle^{-1}$ and $\Lambda_\mathbf{n}(0) = 0$.
- if $\langle \mu\alpha \rangle \geq 1$, then $\Lambda_\mathbf{d} \equiv \Lambda_\mathbf{n}$ and $\Lambda_\mathbf{d}(0) = 1 - \langle \mu/\alpha \rangle^{-1}$.

Moreover, $\Lambda_\mathbf{a}(0) \geq 0$, $\mathbf{a} \in \{\mathbf{n}, \mathbf{d}\}$.

The representation (3.5) provides an expansion of $\Lambda_\mathbf{a}$ into a meromorphic series. However, because the eigenvalues of $\mathcal{A}_\mathbf{a}$ are not necessarily simple, the respective terms of the series (3.5) may have repeated poles. Moreover, in some cases, the coefficients $a_{\mathbf{a},n}$ may vanish. For our purpose, it is more convenient to rewrite the series (3.5) in a form where the poles are different, and the residues do not vanish.

COROLLARY 3.4 (Corollary of Theorem 3.2). *The symbol $\Lambda_\mathbf{a}$, $\mathbf{a} \in \{\mathbf{n}, \mathbf{d}\}$, satisfies*

$$(3.6) \quad \Lambda_\mathbf{a}(\omega) = \Lambda_\mathbf{a}(0) - \sum_{k=1}^{+\infty} \frac{A_{\mathbf{a},k}\omega^2}{\Omega_{\mathbf{a},k}^2 - \omega^2},$$

where the poles $0 < \Omega_{\mathbf{a},0} < \Omega_{\mathbf{a},1} < \dots \rightarrow +\infty$, the coefficients $A_{\mathbf{a},k} > 0$ for all $k \geq 1$, and $\Lambda_\mathbf{a}(0)$ is given in Proposition 3.3. The above series converges uniformly on compact subsets of $\mathbb{C} \setminus \{\pm\Omega_{\mathbf{a},k}, k \in \mathbb{N}_\}$.*

Proof. The proof of (3.6) is immediate from (3.5). By Theorem 3.2 the proof of uniform convergence in $\mathbb{C} \setminus \{\pm\Omega_{\mathbf{a},k}, k \in \mathbb{N}_*\}$ is a matter of verifying that the series converges uniformly in $B_\delta(\pm\omega_{\mathbf{a},n})$, where $\omega_{\mathbf{a},n} > 0$ is not a pole of $\Lambda_\mathbf{a}$, for $\delta > 0$ sufficiently small. This follows by a direct computation, thus we omit the details. \square

3.1.2. Reference DtN in the time domain. The expression (3.6) provides a convenient way to realize the DtN operator in the time domain. In particular, the symbol $\omega \mapsto \frac{i\omega}{\Omega_{\mathbf{a},\ell}^2 - \omega^2}$ corresponds to the following convolution operator:

$$\mathcal{F}\lambda = \frac{i\omega}{\Omega_{\mathbf{a},\ell}^2 - \omega^2} \mathcal{F}g \iff \frac{d^2}{dt^2}\lambda + \Omega_{\mathbf{a},\ell}^2 \lambda = \frac{d}{dt}g, \quad \lambda(0) = \frac{d}{dt}\lambda(0) = 0,$$

where g is sufficiently smooth with $g(0) = g'(0) = 0$. To formalize this result, we need the following assumption on g :

$$(3.7) \quad g \in C^2(\mathbb{R}^+), \quad g(0) = \dots = g^{(2)}(0) = 0, \quad \text{and } g^{(3)} \in L_{loc}^1(\mathbb{R}^+).$$

LEMMA 3.5. *Let g satisfy (3.7). Let $\lambda_{\mathbf{a},\ell}$, $\ell \in \mathbb{N}_*$, solve the system of ODEs:*

$$(3.8) \quad \frac{d^2 \lambda_{\mathbf{a},\ell}}{dt^2} + \Omega_{\mathbf{a},\ell}^2 \lambda_{\mathbf{a},\ell} = \frac{dg}{dt}, \quad \lambda_{\mathbf{a},\ell}(0) = \frac{d\lambda_{\mathbf{a},\ell}}{dt}(0) = 0.$$

Then

(1) the series $\sum_{\ell=1}^{\infty} A_{\mathbf{a},\ell} \lambda'_{\mathbf{a},\ell}(t)$ converges uniformly on compact subsets of \mathbb{R}^+ .

(2) if, additionally, for all $t > 0$, $|g(t)| \leq C(1 + t^n)$, with some C , $n \geq 0$, then

$$(3.9) \quad \Lambda_{\mathbf{a}}(\partial_t)g(t) = \Lambda_{\mathbf{a}}(0)g(t) + \sum_{\ell=1}^{\infty} A_{\mathbf{a},\ell} \lambda'_{\mathbf{a},\ell}(t).$$

Before proving the above, let us state the following technical lemma.

LEMMA 3.6. *The series $S_{\mathbf{a}} = \sum_{\ell=1}^{\infty} A_{\mathbf{a},\ell} \Omega_{\mathbf{a},\ell}^{-2}$ converges.*

Proof. Provided $r \in (0, \Omega_{\mathbf{a},1})$, where $\Omega_{\mathbf{a},1}$ is the smallest positive pole of $\Lambda_{\mathbf{a}}(\omega)$, the series $S_{\mathbf{a},r} := \Lambda_{\mathbf{a}}(r) - \Lambda_{\mathbf{a}}(0) = \sum_{\ell=1}^{\infty} A_{\mathbf{a},\ell} r^2 (\Omega_{\mathbf{a},\ell}^2 - r^2)^{-1}$ converges, according to Corollary 3.4. We conclude by noticing that $|S_{\mathbf{a}}| < r^{-2} S_{\mathbf{a},r}$. \square

Proof of Lemma 3.5. Proof of (1). As $g'(0) = 0$, the solution to (3.8) is given by

$$\lambda_{\mathbf{a},\ell}(t) = \Omega_{\mathbf{a},\ell}^{-1} \int_0^t \sin \Omega_{\mathbf{a},\ell}(t - \tau) g'(\tau) d\tau, \quad \text{and} \quad \lambda'_{\mathbf{a},\ell}(t) = \int_0^t \cos \Omega_{\mathbf{a},\ell}(t - \tau) g'(\tau) d\tau,$$

Next, we re-express $\lambda_{\mathbf{a},\ell}$ so that the general term of the series $\sum_{\ell=1}^{\infty} A_{\mathbf{a},\ell} \lambda'_{\mathbf{a},\ell}$ can be bounded by the general term of the convergent series S , namely $A_{\mathbf{a},\ell} \Omega_{\mathbf{a},\ell}^{-2}$. For this we integrate by parts twice, to obtain

$$(3.10) \quad \lambda'_{\mathbf{a},\ell}(t) = \Omega_{\mathbf{a},\ell}^{-2} g^{(2)}(t) - \Omega_{\mathbf{a},\ell}^{-2} \int_0^t \cos \Omega_{\mathbf{a},\ell}(t - \tau) g^{(3)}(\tau) d\tau,$$

where we used $g^{(1)}(0) = g^{(2)}(0) = 0$. Hence,

$$\sum_{\ell=1}^{\infty} A_{\alpha,\ell} |\lambda'_{\alpha,\ell}(t)| \leq \sum_{\ell=1}^{\infty} \frac{A_{\alpha,\ell}}{\Omega_{\alpha,\ell}^2} \left(|g^{(2)}(t)| + \int_0^t |g^{(3)}(\tau)| d\tau \right).$$

This proves the uniform convergence of $\sum_{\ell=1}^{\infty} A_{\alpha,\ell} |\lambda'_{\alpha,\ell}(t)|$ on compact subsets of \mathbb{R}^+ .

Proof of (2). it suffices to prove that the expression in the right-hand side of (3.9) is $\mathcal{F}^{-1}(\Lambda_{\alpha}(\omega)\mathcal{F}g(\omega))$. This follows by a direct computation, cf. (3.6) (the polynomial bound on g is used to ensure that $\omega \mapsto \mathcal{F}g(\omega)$ is analytic in \mathbb{C}^+). \square

3.1.3. Approximating the reference DtN in the time domain. Based on the results of the previous section, it is natural to approximate the reference DtN operator by truncating the series (3.9) to N terms:

$$(3.11) \quad \Lambda_{\alpha}^N(\partial_t)g(t) = \Lambda_{\alpha}(0)g(t) + \sum_{\ell=1}^N A_{\alpha,\ell} \frac{d\lambda_{\alpha,\ell}}{dt}(t),$$

where $\lambda_{\alpha,\ell}$ are defined in (3.8). The symbol of this operator reads

$$(3.12) \quad \Lambda_{\alpha}^N(\omega) = \Lambda_{\alpha}(0) - \sum_{\ell=1}^N \frac{A_{\alpha,\ell}\omega^2}{\Omega_{\alpha,\ell}^2 - \omega^2}.$$

To show how the error of truncating (3.11) depends on N , let us introduce the following notation for the remainder of the series S_{α} from Lemma 3.6:

$$(3.13) \quad r_{\alpha,N} := \sum_{\ell=N+1}^{\infty} \frac{A_{\alpha,\ell}}{\Omega_{\alpha,\ell}^2}.$$

The error then is quantified by the following lemma.

LEMMA 3.7. *Let g satisfy (3.7) and Lemma 3.5(2). Then*

$$(3.14) \quad |\Lambda_{\alpha}(\partial_t)g(t) - \Lambda_{\alpha}^N(\partial_t)g(t)| \leq 2r_{\alpha,N} \int_0^t |g^{(3)}(\tau)| d\tau, \quad \text{for all } t \geq 0.$$

Proof. Difference of (3.9) and (3.11) yields

$$\begin{aligned} |\Lambda_{\alpha}(\partial_t)g(t) - \Lambda_{\alpha}^N(\partial_t)g(t)| &= \left| \sum_{\ell=N+1}^{\infty} A_{\alpha,\ell} \lambda'_{\alpha,\ell}(t) \right|, \text{ from where, by (3.10),} \\ |\Lambda_{\alpha}(\partial_t)g(t) - \Lambda_{\alpha}^N(\partial_t)g(t)| &\leq \sum_{\ell=N+1}^{\infty} \frac{A_{\alpha,\ell}}{\Omega_{\alpha,\ell}^2} \left(|g^{(2)}(t)| + \int_0^t |g^{(3)}(\tau)| d\tau \right). \end{aligned}$$

We conclude by bounding $|g^{(2)}(t)|$ by $\int_0^t |g^{(3)}(\tau)| d\tau$ (recall that $g^{(2)}(0) = 0$). \square

The above result shows that the error of the truncation of the DtN operator is controlled by the remainder $r_{\alpha,N}$ of the convergent series S , and thus, as $N \rightarrow +\infty$, converges to zero. In the following section we will prove that approximating $\Lambda_{\alpha}(\partial_t)$ by (3.11) in the transparent boundary conditions (2.12) and using the respective approximation in the coupled problem (2.14) leads to a stable problem. Moreover, we will provide a quantification of the solution error.

3.2. An approximate problem on \mathcal{T}^m : formulation and stability.

3.2.1. Formulation. Let us consider (2.14) with $\mathcal{B}_m^a(\partial_t)$ replaced by the truncated DtN operator $\mathcal{B}_m^{a,N}(\partial_t)$, defined as, cf. (2.13),

$$\mathcal{B}_m^{a,N}(\partial_t) = \text{diag} \left(\mathcal{B}_{m,0}^{a,N}(\partial_t), \dots, \mathcal{B}_{m,p^m-1}^{a,N}(\partial_t) \right),$$

where each $\mathcal{B}_{m,j}^{a,N}(\partial_t)$ is expressed via the truncated reference DtN, like in the definition of $\mathcal{B}_{m,j}^a(\partial_t)$ via $\Lambda_a(\partial_t)$, cf. (2.12):

$$(3.15) \quad \mathcal{B}_{m,j}^{a,N}(\partial_t) = \mu_{m,j} \alpha_{m,j}^{-1} \sum_{k=0}^{p-1} \frac{\mu_k}{\alpha_k} \Lambda_a^N(\alpha_k \alpha_{m,j} \partial_t).$$

These are the operators with the following symbols, cf. also (3.12) for $\Lambda_a^N(\omega)$:

$$(3.16) \quad \mathcal{B}_{m,j}^{a,N}(\omega) = \mu_{m,j} \alpha_{m,j}^{-1} \left(\left\langle \frac{\mu}{\alpha} \right\rangle \Lambda_a(0) - \sum_{k=0}^{p-1} \frac{\mu_k}{\alpha_k} \sum_{\ell=1}^N \frac{A_{a,\ell} \omega^2}{(\alpha_{m,j}^{-1} \alpha_k^{-1} \Omega_{a,\ell})^2 - \omega^2} \right).$$

Replacing $\mathcal{B}_m^a(\partial_t)$ in (2.14) by $\mathcal{B}_m^{a,N}(\partial_t)$ leads to the following problem: find

$$u_m^{a,N} \in C^1(\mathbb{R}^+; L_\mu^2(\mathcal{T}^m)) \cap C(\mathbb{R}^+; \mathbf{V}_\mu(\mathcal{T}^m)),$$

s.t. $u_m^{a,N}(\cdot, 0) = \partial_t u_m^{a,N}(\cdot, 0) = 0$, and that satisfies, for all $v \in \mathbf{V}_\mu(\mathcal{T}^m)$, the following:

$$(3.17a) \quad (\partial_t^2 u_m^{a,N}, v)_{\mathcal{T}^m} + (\partial_s u_m^{a,N}, \partial_s v)_{\mathcal{T}^m} + \int_{\Gamma_m} \mathcal{B}_m^{a,N}(\partial_t) \gamma_m u_m^{a,N} \gamma_m v = (f, v)_{\mathcal{T}^m},$$

where $(\mathcal{B}_m^{a,N}(\partial_t) \gamma_m u_m^{a,N}(t)) \in \mathbb{R}^{p^m}$ is defined as follows:

$$(3.17b) \quad \begin{aligned} (\mathcal{B}_m^{a,N}(\partial_t) \gamma_m u_m^{a,N})(t) &= \mathbf{W}_m \mathbf{D}_m \left(\left\langle \frac{\mu}{\alpha} \right\rangle \Lambda_a(0) \gamma_m u_m^{a,N}(t) + \sum_{k=0}^{p-1} \frac{\mu_k}{\alpha_k} \sum_{\ell=1}^N A_{a,\ell} \frac{d\lambda_{\ell,k}}{dt}(t) \right), \\ \mathbf{D}_m &= \text{diag}(\alpha_{m,0}^{-1}, \dots, \alpha_{m,p^m-1}^{-1}), \quad \mathbf{W}_m = \text{diag}(\mu_{m,0}, \dots, \mu_{m,p^m-1}), \end{aligned}$$

and the vector-valued functions $\lambda_{\ell,k} : \mathbb{R}^+ \rightarrow \mathbb{R}^{p^m}$ solve

$$(3.17c) \quad \frac{d^2 \lambda_{\ell,k}}{dt^2} + \alpha_k^{-2} \Omega_{a,\ell}^2 \mathbf{D}_m^2 \lambda_{\ell,k} = \partial_t \gamma_m u_m^{a,N}, \quad \lambda_{\ell,k}(0) = \frac{d\lambda_{\ell,k}}{dt}(0) = 0.$$

3.2.2. Stability of the formulation (3.17). The stability of (3.17) is guaranteed by the non-negativity of $\Lambda_a(0)$, see Proposition 3.3, and of $A_{a,\ell}$ in (3.16), cf. Corollary 3.4. To prove this, we introduce an energy associated with (3.17):

$$E_m^{a,N}(t) := E_{m,u}^{a,N}(t) + E_{m,\lambda}^{a,N}(t), \text{ where}$$

$$(3.18) \quad \begin{aligned} E_{m,u}^{a,N}(t) &:= \frac{1}{2} \left(\|\partial_t u_m^{a,N}(t)\|_{\mathcal{T}^m}^2 + \|\partial_s u_m^{a,N}(t)\|_{\mathcal{T}^m}^2 + \left\langle \frac{\mu}{\alpha} \right\rangle \Lambda_a(0) \int_{\Gamma_m} \frac{\mu}{\alpha} |\gamma_m u_m^{a,N}(t)|^2 \right), \\ E_{m,\lambda}^{a,N}(t) &:= \frac{1}{2} \sum_{k=0}^{p-1} \sum_{\ell=1}^N A_{a,\ell} \frac{\mu_k}{\alpha_k} \left(\int_{\Gamma_m} \frac{\mu}{\alpha} |\partial_t \lambda_{\ell,k}(t)|^2 + \frac{\Omega_{a,\ell}^2}{\alpha_k^2} \int_{\Gamma_m} \frac{\mu}{\alpha^3} |\lambda_{\ell,k}(t)|^2 \right). \end{aligned}$$

THEOREM 3.8 (Stability). *Let $f \in L^1_{loc}(\mathbb{R}^+; L^2_\mu(\mathcal{T}^m))$. Then, for all $T > 0$,*

$$\sqrt{E_m^{\alpha, N}(t)} \leq C \int_0^T \|f(\tau)\|_{L^2_\mu(\mathcal{T}^m)} d\tau, \quad \text{for all } 0 \leq t \leq T,$$

where $C > 0$ does not depend on N, m, T, α, μ .

Proof. The proof is classical. It suffices to test (3.17a) with $v = \partial_t u_m^{\alpha, N}$. Then, by (3.17c), with $\langle \cdot, \cdot \rangle$ denoting the Euclidean scalar product in \mathbb{R}^{p^m} ,

$$\langle \mathbf{W}_m \mathbf{D}_m \partial_t \lambda_{\ell, k}, \partial_t \gamma_m u_m^{\alpha, N} \rangle = \frac{1}{2} \frac{d}{dt} \left(\int_{\Gamma_m} \frac{\mu}{\alpha} |\partial_t \lambda_{\ell, k}(t)|^2 + \alpha_k^{-2} \Omega_{\alpha, \ell}^2 \int_{\Gamma_m} \frac{\mu}{\alpha^3} |\lambda_{\ell, k}(t)|^2 \right).$$

This results in the energy identity $\frac{d}{dt} E_m^{\alpha, N} = (f, \partial_t u_m^{\alpha, N})_{\mathcal{T}^m}$. The rest follows by a straightforward application of a Gronwall's lemma, cf. [7, Appendix E]. \square

3.3. Error analysis. Here we study the error of approximating (2.14) by (3.17) as a function of the number of the terms in the truncated series N , as $N \rightarrow \infty$. Let us introduce the following energy norm of $v \in C^0(\mathbb{R}^+; \mathbf{V}_\mu(\mathcal{T}^m)) \cap C^1(\mathbb{R}^+; L^2_\mu(\mathcal{T}^m))$:

$$\|v\|_{[0, T]; \mathcal{T}^m} := \sup_{t \leq T} (\|\partial_t v(\cdot, t)\|_{\mathcal{T}^m} + \|\partial_s v(\cdot, t)\|_{\mathcal{T}^m}).$$

Let us also introduce the error

$$(3.19) \quad \varepsilon_m^{\alpha, N} := u_m^{\alpha, N} - u_m^\alpha \quad (\text{recall that } u_m^{\alpha, N} = u_\alpha|_{\mathcal{T}^m} \text{ by Theorem 2.10}).$$

The principal result of this section is summarized below.

THEOREM 3.9. *Let $m, N \geq 1$. Let $f \in W^{4,1}_{loc}(\mathbb{R}^+; L^2_\mu(\mathcal{T}^m))$ be s.t. $f^{(j)}(0) = 0$, $j = 0, \dots, 3$, and satisfy Assumption 2.8. Then, with $r_{\alpha, N}$ defined in (3.13), the error (3.19) satisfies for all $T > 0$,*

$$(3.20) \quad \|\varepsilon_m^{\alpha, N}\|_{[0, T]; \mathcal{T}^m} \leq C_m r_{\alpha, N} T \|\partial_t^4 \partial_s u\|_{L^1(0, T; L^2_\mu(\mathcal{T}))},$$

where $C_m > 0$ is given by

$$C_m = \begin{cases} C m^2 \eta^m, & \eta = \max(\langle \mu \alpha \rangle, |\alpha|_\infty^2), & \text{if } \langle \mu \alpha \rangle < 1, \\ C |\alpha|_\infty^{2m}, & & \text{if } \langle \mu \alpha \rangle \geq 1, \end{cases}$$

and the constant $C > 0$ does not depend on T, m, N .

Therefore, for fixed T, m , $\|\varepsilon_m^{\alpha, N}(T)\|_{L^2_\mu(\mathcal{T}^m)} \rightarrow 0$, as $N \rightarrow +\infty$.

REMARK 3.10. *Theorem 3.9 indicates as well the behaviour of the error $\varepsilon_m^{\alpha, N}$ as a function of m (the level at which the tree is truncated). First, remark that the respective bound can be translated as a bound for $\|\varepsilon_m^{\alpha, N}(t)\|_{L^2_\mu(\mathcal{T}^m)}$: since $\varepsilon_m^{\alpha, N}(0) = 0$, we have*

$$(3.21) \quad \|\varepsilon_m^{\alpha, N}(t)\|_{\mathcal{T}^m} \leq t \sup_{\tau \in (0, t)} \|\partial_\tau \varepsilon_m^{\alpha, N}(\tau)\|_{\mathcal{T}^m}.$$

Therefore, when N, T are fixed, as $m \rightarrow \infty$, $\|\varepsilon_m^{\alpha, N}(T)\|_{L^2_\mu(\mathcal{T}^m)} \rightarrow 0$.

We consider that this is of less importance than the error bound with respect to N , because the complexity of the resolution of (3.17) increases exponentially with m , since at each generation there are p^m edges. Concurrently, this complexity is linear in N .

The proof of Theorem 3.9 relies on two auxiliary trace lemmas that follow from [9].

LEMMA 3.11. *Let $v \in \mathbf{V}_\mu(\mathcal{T}^m)$. Then, for all $m \geq 1$,*

$$(3.22) \quad \int_{\Gamma_m} \boldsymbol{\mu} \boldsymbol{\alpha} |\gamma_m v|^2 \leq C_{\boldsymbol{\alpha}, \boldsymbol{\mu}} m^2 \eta^m \|\partial_s v\|_{L_\mu^2(\mathcal{T}^m)}^2, \quad \eta = \max(\langle \boldsymbol{\mu} \boldsymbol{\alpha} \rangle, |\boldsymbol{\alpha}|_\infty^2),$$

where $C_{\boldsymbol{\alpha}, \boldsymbol{\mu}} > 0$ is independent of m .

Proof. The proof relies on the following inequality from the proof of [9, Theorem 3.24] (in the notation of [9], see also (117), $\int_{\Gamma_m} \boldsymbol{\mu} \boldsymbol{\alpha} |\gamma_m v|^2 = \|\Pi v\|_{L_\mu^2(\mathcal{G}^m)}^2$):

$$\int_{\Gamma_m} \boldsymbol{\mu} \boldsymbol{\alpha} |\gamma_m v|^2 \leq C_m \|\partial_s v\|_{L_\mu^2(\mathcal{T}^m)}^2, \quad C_m = \begin{cases} m^2 \langle \boldsymbol{\mu} \boldsymbol{\alpha} \rangle^m & \text{if } \langle \boldsymbol{\mu} \boldsymbol{\alpha} \rangle = |\boldsymbol{\alpha}|_\infty^2, \\ m |\boldsymbol{\alpha}|_\infty^2 \frac{\langle \boldsymbol{\mu} \boldsymbol{\alpha} \rangle^m - |\boldsymbol{\alpha}|_\infty^{2m}}{\langle \boldsymbol{\mu} \boldsymbol{\alpha} \rangle - |\boldsymbol{\alpha}|_\infty^2}, & \text{if } \langle \boldsymbol{\mu} \boldsymbol{\alpha} \rangle \neq |\boldsymbol{\alpha}|_\infty^2. \end{cases}$$

The result follows with $C_m \leq C m^2 \max(\langle \boldsymbol{\mu} \boldsymbol{\alpha} \rangle^m, |\boldsymbol{\alpha}|_\infty^{2m})$, $C > 0$. \square

LEMMA 3.12. *Let $\langle \boldsymbol{\mu} \boldsymbol{\alpha} \rangle \geq 1$, and $v \in \mathbf{H}_\mu^1(\mathcal{T}) = \mathbf{H}_{\mu,0}^1(\mathcal{T})$. Then, for all $m \geq 1$,*

$$(3.23) \quad \int_{\Gamma_m} \boldsymbol{\mu} \boldsymbol{\alpha}^{-1} |\gamma_m v|^2 \leq C_{\boldsymbol{\alpha}, \boldsymbol{\mu}} \|\partial_s v\|_{L_\mu^2(\mathcal{T})}^2,$$

where $C_{\boldsymbol{\alpha}, \boldsymbol{\mu}}$ is independent of m .

Proof. See [9, the end of the proof of Theorem 3.18 and the notation (110)]. \square

Proof of Theorem 3.9. First, we remark that the regularity condition on f ensures the required regularity of the solution u_α , see [6]. Let us fix N, m .

Step 1. Re-expressing $\varepsilon_m^{\alpha, N}$. By taking difference between (3.17) and (2.14), we see that the error $\varepsilon_m^{\alpha, N}$ solves the following problem:

find $\varepsilon_m^{\alpha, N} \in C^0(\mathbb{R}^+; \mathbf{V}_\mu(\mathcal{T}^m))$, s.t. $\varepsilon_m^{\alpha, N}(0) = \partial_t \varepsilon_m^{\alpha, N}(0) = 0$, and

$$(\partial_t^2 \varepsilon_m^{\alpha, N}, v)_{\mathcal{T}^m} + (\partial_s \varepsilon_m^{\alpha, N}, \partial_s v)_{\mathcal{T}^m} + \int_{\Gamma_m} (\mathcal{B}_m^{\alpha, N}(\partial_t) \gamma_m u_m^{\alpha, N} - \mathcal{B}_m^\alpha(\partial_t) \gamma_m u_\alpha) \gamma_m v = 0,$$

for all $v \in \mathbf{V}_\mu(\mathcal{T}^m)$. Defining

$$(3.24) \quad \zeta_m^{\alpha, N} = (\mathcal{B}_m^\alpha(\partial_t) - \mathcal{B}_m^{\alpha, N}(\partial_t)) \gamma_m u_\alpha,$$

we rewrite the above in the form (3.17a):

$$(\partial_t^2 \varepsilon_m^{\alpha, N}, v)_{\mathcal{T}^m} + (\partial_s \varepsilon_m^{\alpha, N}, \partial_s v)_{\mathcal{T}^m} + \int_{\Gamma_m} \mathcal{B}_m^{\alpha, N}(\partial_t) \gamma_m \varepsilon_m^{\alpha, N} \gamma_m v = \int_{\Gamma_m} \zeta_m^{\alpha, N} \gamma_m v.$$

To derive the error estimates, we will use the energy techniques, like in Theorem 3.8. Let us introduce an energy of the error, cf. the definition (3.18),

$$(3.25) \quad \mathcal{E} := \frac{1}{2} \left(\|\partial_t \varepsilon_m^{\alpha, N}\|_{\mathcal{T}^m}^2 + \|\partial_s \varepsilon_m^{\alpha, N}\|_{\mathcal{T}^m}^2 + \left\langle \frac{\boldsymbol{\mu}}{\boldsymbol{\alpha}} \right\rangle \Lambda_\alpha(0) \int_{\Gamma_m} \frac{\boldsymbol{\mu}}{\boldsymbol{\alpha}} |\gamma_m \varepsilon_m^{\alpha, N}|^2 \right) + \mathcal{E}_\lambda,$$

with \mathcal{E}_λ defined like in (3.18). Like in the proof of Theorem 3.8, we have

$$(3.26) \quad \frac{d}{dt} \mathcal{E}(t) = \int_{\Gamma_m} \zeta_m^{\mathbf{a},N}(t) \partial_t \gamma_m \varepsilon_m^{\mathbf{a},N}(t).$$

Integrating the above from 0 to T results in (since $\varepsilon_m^{\mathbf{a},N}(0) = \partial_t \varepsilon_m^{\mathbf{a},N}(0) = 0$):

$$(3.27) \quad \mathcal{E}(T) = \underbrace{\int_{\Gamma_m} \zeta_m^{\mathbf{a},N}(T) \gamma_m \varepsilon_m^{\mathbf{a},N}(T)}_{I_1(T)} - \underbrace{\int_0^T \int_{\Gamma_m} \partial_t \zeta_m^{\mathbf{a},N}(t) \gamma_m \varepsilon_m^{\mathbf{a},N}(t) dt}_{I_2(T)}.$$

Step 2. Bounding the right-hand side of (3.27).

Step 2.1. Bounding $I_1(T)$. From (3.24) and the representation (3.15), it follows

$$|I_1(T)| \leq \sum_{k=0}^{p-1} \frac{\mu_k}{\alpha_k} \int_{\Gamma_m} \left(\frac{\mu}{\alpha} |\Lambda_{\mathbf{a}}^N(\alpha_k \boldsymbol{\alpha} \partial_t) \gamma_m u_{\mathbf{a}}(T) - \Lambda_{\mathbf{a}}(\alpha_k \boldsymbol{\alpha} \partial_t) \gamma_m u_{\mathbf{a}}(T)| |\gamma_m \varepsilon_m^{\mathbf{a},N}(T)| \right).$$

The goal is to find a bound for the above by bounding (cf. the notation (2.6))

$$(3.28) \quad q_{m,j}(t) := \Lambda_{\mathbf{a}}^N(\alpha_k \alpha_{m,j} \partial_t) u_{\mathbf{a}}(M_{m,j}, t) - \Lambda_{\mathbf{a}}(\alpha_k \alpha_{m,j} \partial_t) u_{\mathbf{a}}(M_{m,j}, t).$$

Since $\Lambda_{\mathbf{a}}(\alpha_k \alpha_{m,j} \omega) = \Lambda_{\mathbf{a}}(0) - \sum_{\ell=1}^{\infty} \frac{A_{\mathbf{a},\ell} \omega^2}{(\alpha_k^{-1} \alpha_{m,j}^{-1} \Omega_{\mathbf{a},\ell})^2 - \omega^2}$, to bound $q_{m,j}$, we use the same argument as in (3.14), see also (3.13):

$$\begin{aligned} |q_{m,j}(t)| &\leq \sum_{\ell=N+1}^{\infty} \frac{A_{\mathbf{a},\ell}}{\alpha_k^{-2} \alpha_{m,j}^{-2} \Omega_{\mathbf{a},\ell}^2} \|\partial_\tau^3 u_{\mathbf{a}}(M_{m,j}, \cdot)\|_{L^1(0,t)} \\ &= \alpha_k^2 \alpha_{m,j}^2 r_{\mathbf{a},N} \|\partial_\tau^3 u_{\mathbf{a}}(M_{m,j}, \cdot)\|_{L^1(0,t)}. \end{aligned}$$

Therefore,

$$(3.29) \quad \begin{aligned} |I_1(T)| &\leq 2r_{\mathbf{a},N} \sum_{k=0}^{p-1} \frac{\mu_k}{\alpha_k} \int_0^T \int_{\Gamma_m} \left(\frac{\mu}{\alpha} \alpha_k^2 \alpha^2 |\partial_\tau^3 \gamma_m u_{\mathbf{a}}(\tau)| |\gamma_m \varepsilon_m^{\mathbf{a},N}(T)| \right) d\tau \\ &= 2r_{\mathbf{a},N} \langle \boldsymbol{\mu} \boldsymbol{\alpha} \rangle \int_0^T \int_{\Gamma_m} \left(\boldsymbol{\mu} \boldsymbol{\alpha} |\partial_\tau^3 \gamma_m u_{\mathbf{a}}(\tau)| |\gamma_m \varepsilon_m^{\mathbf{a},N}(T)| \right) d\tau. \end{aligned}$$

Step 2.2. Bounding $I_2(T)$. The same argument as in Step 2.1 yields

$$(3.30) \quad \begin{aligned} \left| \int_{\Gamma_m} \partial_t \zeta_m^{\mathbf{a},N}(t) \gamma_m \varepsilon_m^{\mathbf{a},N}(t) \right| &\leq 2r_{\mathbf{a},N} \langle \boldsymbol{\mu} \boldsymbol{\alpha} \rangle \int_0^t \int_{\Gamma_m} \left(\boldsymbol{\mu} \boldsymbol{\alpha} |\partial_\tau^4 \gamma_m u_{\mathbf{a}}(\tau)| |\gamma_m \varepsilon_m^{\mathbf{a},N}(t)| \right) d\tau, \text{ thus} \\ |I_2(T)| &\leq 2r_{\mathbf{a},N} \langle \boldsymbol{\mu} \boldsymbol{\alpha} \rangle \int_0^T \int_0^t \int_{\Gamma_m} \left(\boldsymbol{\mu} \boldsymbol{\alpha} |\partial_\tau^4 \gamma_m u_{\mathbf{a}}(\tau)| |\gamma_m \varepsilon_m^{\mathbf{a},N}(t)| \right) d\tau dt. \end{aligned}$$

Step 2.3. Bounding the right-hand side of (3.27). We use the bounds (3.29) and (3.30) to bound (3.27) as follows:

$$\begin{aligned}
\mathcal{E}(T) &\leq 2r_{\alpha,N} \langle \mu \alpha \rangle \int_0^T \int_{\Gamma_m} \left(\mu \alpha |\partial_\tau^3 \gamma_m u_a(\tau)| |\gamma_m \varepsilon_m^{\alpha,N}(T)| \right) d\tau \\
&\quad + 2r_{\alpha,N} \langle \mu \alpha \rangle \int_0^T \int_0^t \int_{\Gamma_m} \left(\mu \alpha |\partial_\tau^4 \gamma_m u_a(\tau)| |\gamma_m \varepsilon_m^{\alpha,N}(t)| \right) d\tau dt \\
(3.31) \quad &\leq 2r_{\alpha,N} \langle \mu \alpha \rangle \int_0^T \int_0^t \int_{\Gamma_m} \left(\mu \alpha |\partial_\tau^4 \gamma_m u_a(\tau)| (|\gamma_m \varepsilon_m^{\alpha,N}(T)| + |\gamma_m \varepsilon_m^{\alpha,N}(t)|) \right) d\tau dt,
\end{aligned}$$

where in the last bound we used $\partial_\tau^3 \gamma_m u_a = \int_0^t \partial_\tau^4 \gamma_m u_a$ (it holds that $\partial_t^3 \gamma_m u_a|_{t=0} = 0$ because of the finite speed of wave propagation and the assumption on the source f).

Step 3. Bounding $\varepsilon_m^{\alpha,N}$ based on (3.31). Naturally, we would like to apply a Gronwall inequality to the bound (3.31). The cases $\langle \mu \alpha \rangle < 1$ and $\langle \mu \alpha \rangle \geq 1$ will be treated differently. When $\langle \mu \alpha \rangle < 1$, by Theorem 2.7 and Proposition 3.3,

- (1) if $\langle \mu \alpha \rangle > 1$, then $\Lambda_\partial \neq \Lambda_n$, $\Lambda_\partial(0) > 0$ and $\Lambda_n(0) = 0$.
- (2) if $\langle \mu \alpha \rangle \leq 1$, then $\Lambda_n = \Lambda_\partial$, $\Lambda_\partial(0) = \Lambda_n(0) = 0$.

Let us consider the case (2). As $\Lambda_a(0) = 0$, the boundary term in (3.25) vanishes, and does not control $\gamma_m \varepsilon_m^{\alpha,N}(T)$. Hence instead we will use the trace continuity result of Lemma 3.11. Because this strategy will allow to conclude that the error decays exponentially fast in m , we will make use of it also in the case (1), when $\Lambda_a(0)$ does not necessarily vanish (i.e. when $\Lambda = \Lambda_\partial$).

The obtained error bound is still valid when $\langle \mu \alpha \rangle \geq 1$, but it is non-optimal (it grows exponentially fast with m). That is why we deal with the case $\langle \mu \alpha \rangle \geq 1$ separately. Here, by Theorem 2.7 and Proposition 3.3, $\Lambda_\partial = \Lambda_n$, $\Lambda_a(0) > 0$. This property allows to control the $\gamma_m \varepsilon_m^{\alpha,N}$ by the energy \mathcal{E} .

Error bound when $\langle \mu \alpha \rangle < 1$. Application of the Cauchy-Schwarz inequality to both terms of (3.31) yields

$$\begin{aligned}
\mathcal{E}(T) &\leq 2r_{\alpha,N} \langle \mu \alpha \rangle \int_0^T \int_0^t \left(\int_{\Gamma_m} \mu \alpha |\partial_\tau^4 \gamma_m u_a(\tau)|^2 \right)^{\frac{1}{2}} \left(\int_{\Gamma_m} \mu \alpha |\gamma_m \varepsilon_m^{\alpha,N}(T)|^2 \right)^{\frac{1}{2}} d\tau dt \\
&\quad + 2r_{\alpha,N} \langle \mu \alpha \rangle \int_0^T \int_0^t \left(\int_{\Gamma_m} \mu \alpha |\partial_\tau^4 \gamma_m u_a(\tau)|^2 \right)^{\frac{1}{2}} \left(\int_{\Gamma_m} \mu \alpha |\gamma_m \varepsilon_m^{\alpha,N}(t)|^2 \right)^{\frac{1}{2}} d\tau dt.
\end{aligned}$$

Next, we apply (3.22) to the terms with $\gamma_m u_a$ and $\gamma_m \varepsilon_m^{\alpha,N}$, which yields, with $C' > 0$,

$$\begin{aligned}
\mathcal{E}(T) &\leq C' r_{\alpha,N} m^2 \eta^m \int_0^T \int_0^t \|\partial_s \partial_\tau^4 u_a(\tau)\|_{\mathcal{T}^m} d\tau \left(\|\partial_s \varepsilon_m^{\alpha,N}(T)\|_{\mathcal{T}^m} + \|\partial_s \varepsilon_m^{\alpha,N}(t)\|_{\mathcal{T}^m} \right) dt \\
&\leq \sqrt{2} C' r_{\alpha,N} m^2 \eta^m \int_0^T \|\partial_s \partial_t^4 u_a\|_{L^1(0,t;L_\mu^2(\mathcal{T}^m))} \left(\sqrt{\mathcal{E}(T)} + \sqrt{\mathcal{E}(t)} \right) dt.
\end{aligned}$$

A Gronwall's inequality, cf. [7, Appendix E] yields, with $C > 0$ (independent of T):

$$(3.32) \quad \sqrt{\mathcal{E}(T)} \leq Cr_{\mathbf{a},N} m^2 \eta^m \int_0^T \|\partial_s \partial_t^4 u_{\mathbf{a}}\|_{L^1(0,t;L_\mu^2(\mathcal{T}^m))} dt,$$

hence the bound (3.20) in the statement of the theorem.

Error bound when $\langle \mu \alpha \rangle \geq 1$. Like before, we start by applying the Cauchy-Schwarz inequality to (3.31):

$$(3.33) \quad \begin{aligned} \mathcal{E}(T) &\leq 2r_{\mathbf{a},N} \langle \mu \alpha \rangle \int_0^T \int_0^t \left(\int_{\Gamma_m} \mu \alpha^3 |\partial_\tau^3 \gamma_m u_{\mathbf{a}}(\tau)|^2 \right)^{\frac{1}{2}} \left(\int_{\Gamma_m} \mu \alpha^{-1} |\gamma_m \varepsilon_m^{\mathbf{a},N}(T)|^2 \right)^{\frac{1}{2}} d\tau dt \\ &+ 2r_{\mathbf{a},N} \langle \mu \alpha \rangle \int_0^T \int_0^t \left(\int_{\Gamma_m} \mu \alpha^3 |\partial_\tau^4 \gamma_m u_{\mathbf{a}}(\tau)|^2 \right)^{\frac{1}{2}} \left(\int_{\Gamma_m} \mu \alpha^{-1} |\gamma_m \varepsilon_m^{\mathbf{a},N}(t)|^2 \right)^{\frac{1}{2}} d\tau dt. \end{aligned}$$

Remark that, cf. (2.6),

$$\int_{\Gamma_m} \mu \alpha^3 |\partial_\tau^4 \gamma_m u_{\mathbf{a}}|^2 \leq \max_j \alpha_{m,j}^4 \int_{\Gamma_m} \mu \alpha^{-1} |\partial_\tau^4 \gamma_m u_{\mathbf{a}}|^2 \leq |\alpha|_\infty^{4m} \int_{\Gamma_m} \mu \alpha^{-1} |\partial_\tau^4 \gamma_m u_{\mathbf{a}}|^2.$$

Applying Lemma 3.12 to bound the above, we obtain

$$(3.34) \quad \int_{\Gamma_m} \mu \alpha^3 |\partial_\tau^4 \gamma_m u_{\mathbf{a}}|^2 \leq C_{\alpha,\mu}^2 |\alpha|_\infty^{4m} \|\partial_s \partial_\tau^4 u_{\mathbf{a}}\|^2.$$

Moreover, cf. (3.26),

$$\int_{\Gamma_m} \mu \alpha^{-1} |\gamma_m \varepsilon_m^{\mathbf{a},N}(t)|^2 \leq 2 \langle \mu / \alpha \rangle^{-1} \Lambda_{\mathbf{a}}^{-1}(0) \mathcal{E}(t).$$

Thus, with the above and (3.34), the inequality (3.33) can be rewritten as follows:

$$\mathcal{E}(T) \leq Cr_{\mathbf{a},N} |\alpha|_\infty^{2m} \int_0^T \int_0^\tau \|\partial_s \partial_\tau^4 u_{\mathbf{a}}(\tau)\|_{\mathcal{T}^m} d\tau \left(\mathcal{E}^{\frac{1}{2}}(t) + \mathcal{E}^{\frac{1}{2}}(T) \right) dt.$$

To obtain the desired estimate (3.20) we proceed like in the derivation of (3.32):

$$\sqrt{\mathcal{E}(T)} \leq Cr_{\mathbf{a},N} |\alpha|_\infty^{2m} T \|\partial_s \partial_t^4 u_{\mathbf{a}}\|_{L^1(0,T;L_\mu^2(\mathcal{T}^m))}.$$

Step 4. Convergence. Since $\lim_{N \rightarrow +\infty} r_{\mathbf{a},N} = 0$ as a remainder of the convergent series, cf. Lemma 3.6 and (3.13), by combining (3.20) and (3.21), we see that for fixed T, m , it holds that $\lim_{N \rightarrow +\infty} \|\varepsilon_m^{\mathbf{a},N}(T)\|_{\mathcal{T}^m} = 0$. \square

4. Error control and complexity estimates. All over the section we fix the simulation time T and the parameter m and study the behavior of the error with N .

4.1. Error control. It appears that the error bound provided by Theorem 3.9 is (at least partially) computable. Let us show how

$$r_{\mathfrak{a},N} = \sum_{k=N+1}^{\infty} A_{\mathfrak{a},k} \Omega_{\mathfrak{a},k}^{-2}, \quad \mathfrak{a} \in \{\mathfrak{d}, \mathfrak{n}\}, \text{ cf. definition (3.13)},$$

which controls the error, can be approximated numerically, provided that $A_{\mathfrak{a},k}$, $\Omega_{\mathfrak{a},k}$, $k = 1, \dots, N$, are known (see Section 5.1). A direct computation using (3.6) yields

$$\Lambda_{\mathfrak{a}}''(0) = -2 \sum_{k=0}^{\infty} A_{\mathfrak{a},k} \Omega_{\mathfrak{a},k}^{-2}.$$

By Lemma 5.5 and Corollary 5.6 in [9], the left-hand side of the above is known explicitly. Introducing

$$\lambda_{\mathcal{N}} = -(1 - \langle \mu/\alpha \rangle)^{-1}, \quad \lambda_{\mathcal{D}} = -\frac{1}{3} (\langle \mu/\alpha \rangle^2 + \langle \mu/\alpha \rangle + 1) (\langle \mu/\alpha \rangle^2 - \langle \mu/\alpha \rangle)^{-1},$$

we have the following:

- when $\langle \mu/\alpha \rangle \leq 1$, $\Lambda_{\mathfrak{n}}''(0) = \Lambda_{\mathfrak{d}}''(0) = \lambda_{\mathcal{N}}$;
- when $\langle \mu/\alpha \rangle < 1 < \langle \mu/\alpha \rangle$, $\Lambda_{\mathfrak{n}}''(0) = \lambda_{\mathcal{N}}$ and $\Lambda_{\mathfrak{d}}''(0) = \lambda_{\mathcal{D}}$;
- when $\langle \mu/\alpha \rangle \geq 1$, $\Lambda_{\mathfrak{n}}''(0) = \Lambda_{\mathfrak{d}}''(0) = \lambda_{\mathcal{D}}$.

Hence, provided $A_{\mathfrak{a},k}$ and $\Omega_{\mathfrak{a},k}$, $k = 1, \dots, N$ (approximated numerically), we compute

$$r_{\mathfrak{a},N} = -\frac{1}{2} \left(\Lambda_{\mathfrak{a}}''(0) + 2 \sum_{k=1}^N \frac{A_{\mathfrak{a},k}}{\Omega_{\mathfrak{a},k}^2} \right), \quad \mathfrak{a} \in \{\mathfrak{d}, \mathfrak{n}\},$$

with $\Lambda_{\mathfrak{a}}''(0)$ being given by one of the above expressions.

4.2. Convergence and complexity estimates. The complexity of the method described in Section 3 depends linearly on the number of poles N in (3.17). The estimate of Theorem 3.9 shows that in order to ensure that the error in the energy norm is $O(\varepsilon)$, one should choose $N = N_{\mathfrak{a},\varepsilon}$, so that $r_{\mathfrak{a},N} < \varepsilon$. Let

$$(4.1) \quad N_{\mathfrak{a},\varepsilon} := \min_{N \in \mathbb{N}_*} \{r_{\mathfrak{a},N} < \varepsilon\}.$$

In [8] it was shown that $N_{\mathfrak{a},\varepsilon}$ is related to the following quantity:

$$(4.2) \quad P_{\mathfrak{a}}(\lambda) := \#\{k : 0 < \Omega_{\mathfrak{a},k} < \lambda\}.$$

More precisely, $N_{\mathfrak{a},\varepsilon}$ is bounded by

$$(4.3) \quad P_{\mathfrak{a}}(C_1 \varepsilon^{-1}) \leq N_{\mathfrak{a},\varepsilon} \leq P_{\mathfrak{a}}(C_2 \varepsilon^{-1}), \quad \text{with some } C_2 > C_1 > 0.$$

4.2.1. Asymptotic estimates on $N_{\mathfrak{a},\varepsilon}$ and $r_{\mathfrak{a},N}$. As shown by (4.3), to find an asymptotic upper bound on $N_{\mathfrak{a},\varepsilon}$, it is sufficient to obtain a bound on $P_{\mathfrak{a}}(\lambda)$ as $\lambda \rightarrow +\infty$. For this, in [8] we used the fact that the poles in (3.6) are related to the eigenvalues $\omega_{\mathfrak{a},k}$ of $\mathcal{A}_{\mathfrak{a}}$, cf. Theorem 3.2. More precisely, because the eigenvalues $\omega_{\mathfrak{a},k}$ (unlike the poles $\Omega_{\mathfrak{a},k}$) are counted with multiplicities, it holds that $P_{\mathfrak{a}}(\lambda) \leq \#\{k :$

$\omega_{\mathbf{a},k} < \lambda\}$. This allows to relate bounds of $P_{\mathbf{a}}$ to the asymptotics of the eigenvalue counting function. It is then not surprising that such a bound will depend on the geometry of the tree \mathcal{T} . To state it, we define (with $\sum \equiv \sum_i$):

$$(4.4) \quad d_s \in (0, \infty) \text{ a unique number s.t. } \sum \alpha_i^{d_s} = 1.$$

The existence and uniqueness of d_s follows by noticing that $(0, \infty) \ni x \mapsto \sum \alpha_i^x$ is a strictly monotonically decreasing function with the values on the interval $(0, p)$.

To state a bound on $P_{\mathbf{a}}$, let us introduce $\langle \boldsymbol{\alpha} \rangle = \sum \alpha_i$.

THEOREM 4.1 ([8]). *There exists $C_{\mathbf{a}} > 0$, $\mathbf{a} \in \{\mathbf{n}, \mathfrak{d}\}$, depending on $\boldsymbol{\alpha}$, $\boldsymbol{\mu}$, s.t., for all $\lambda > 2$, it holds:*

1. *if $\langle \boldsymbol{\alpha} \rangle < 1$ ($d_s < 1$), then $P_{\mathbf{a}}(\lambda) \leq C_{\mathbf{a}}\lambda$.*
2. *if $\langle \boldsymbol{\alpha} \rangle = 1$ ($d_s = 1$), then $P_{\mathbf{a}}(\lambda) \leq C_{\mathbf{a}}\lambda \log \lambda$.*
3. *if $\langle \boldsymbol{\alpha} \rangle > 1$ ($d_s > 1$), then $P_{\mathbf{a}}(\lambda) \leq C_{\mathbf{a}}\lambda^{d_s}$.*

With the above theorem and (4.3), we can obtain an upper bound on the number of poles in the approximation (3.16) required to achieve a desired accuracy ε .

THEOREM 4.2 ([8]). *There exists $C_{\mathbf{a}}^+ > 0$, depending only on $\boldsymbol{\mu}$, $\boldsymbol{\alpha}$, such that, for all $0 < \varepsilon < 1/2$, $N_{\mathbf{a},\varepsilon}$ satisfies:*

- *if $\langle \boldsymbol{\alpha} \rangle < 1$ ($d_s < 1$), $N_{\mathbf{a},\varepsilon} \leq C_{\mathbf{a}}^+ \varepsilon^{-1}$.*
- *if $\langle \boldsymbol{\alpha} \rangle = 1$ ($d_s = 1$), $N_{\mathbf{a},\varepsilon} \leq C_{\mathbf{a}}^+ \varepsilon^{-1} \log \varepsilon^{-1}$.*
- *if $\langle \boldsymbol{\alpha} \rangle > 1$ ($d_s > 1$), $N_{\mathbf{a},\varepsilon} \leq C_{\mathbf{a}}^+ \varepsilon^{-d_s}$.*

Next, we present a bound on $r_{\mathbf{a},N}$ with respect to N , which, together with the results of Theorem 3.9 allows to conclude about the convergence of the method. This bound is a corollary of Theorem 4.2.

THEOREM 4.3 ([8]). *There exists $c_{\mathbf{a}}^+ > 0$, depending only on $\boldsymbol{\mu}$, $\boldsymbol{\alpha}$, such that, for all $N \geq 2$, $r_{\mathbf{a},N}$ satisfies:*

- *if $\langle \boldsymbol{\alpha} \rangle < 1$ ($d_s < 1$), $r_{\mathbf{a},N} \leq c_{\mathbf{a}}^+ N^{-1}$.*
- *if $\langle \boldsymbol{\alpha} \rangle = 1$ ($d_s = 1$), $r_{\mathbf{a},N} \leq c_{\mathbf{a}}^+ N^{-1} \log N$.*
- *if $\langle \boldsymbol{\alpha} \rangle > 1$ ($d_s > 1$), $r_{\mathbf{a},N} \leq c_{\mathbf{a}}^+ N^{-\frac{1}{d_s}}$.*

The following result provides a lower bound on $P_{\mathbf{a}}$, $N_{\mathbf{a},\varepsilon}$ and $r_{\mathbf{a},N}$.

PROPOSITION 4.4 ([8]). *With some $c_P, c_n, c_r > 0$, $\varepsilon_0, \lambda_0 > 0$, $N_0 \in \mathbb{N}_*$, it holds: for all $\varepsilon < \varepsilon_0$, $\lambda > \lambda_0$, $N > N_0$,*

$$P_{\mathbf{a}}(\lambda) > c_P \lambda, \text{ and, by (4.3), } N_{\mathbf{a},\varepsilon} > c_n \varepsilon^{-1}, \quad r_{\mathbf{a},N} > c_r N^{-1}.$$

The above result shows that the upper bound of Theorems 4.1, 4.2, 4.2, in the case when $\langle \boldsymbol{\alpha} \rangle < 1$, is sharp. When $\langle \boldsymbol{\alpha} \rangle \geq 1$, the sharpness of the upper bounds is not clear, and a numerical investigation is needed.

REMARK 4.5. *Since the error bound provided in Theorem 3.9 is only an upper bound, the lower bound on $r_{\mathbf{a},N}$ given in Proposition 4.4 **does not imply** that the convergence of the method is at best $O(N^{-1})$. Nonetheless, in practice, as we will see in Section 5.3, the bound of Theorem 3.9 is close to optimal.*

4.2.2. Numerical experiments. The goal of this section is to examine numerically the sharpness of the bounds of Theorem 4.1, as this is equivalent, by (4.3), see also [8], to verifying the sharpness of estimates of Theorems 4.2, 4.3. For this we compute the quantity $P_a(\lambda)$ defined in (4.2); the poles of $\Lambda_a(\omega)$ are determined with the help of the method described in Section 5.1. We consider three cases.

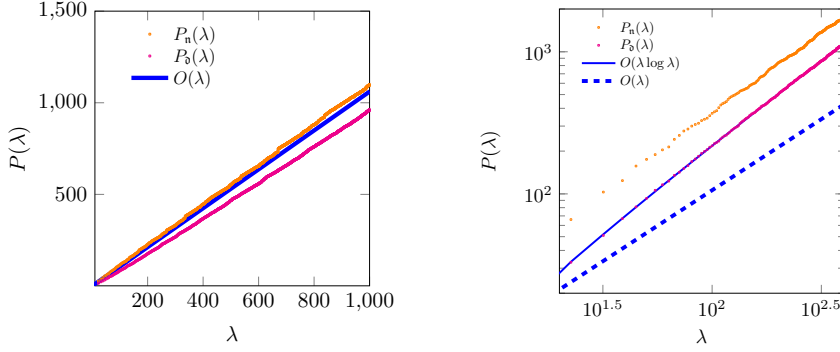


FIGURE 2. $P_a(\lambda)$ vs its theoretical bounds given by Theorem 4.1 and Proposition 4.4 for the case when $\sum \alpha_i \leq 1$. Left: $\alpha = (0.5, 0.2)$, $\mu = (1, 2)$. Right: $\alpha = (0.6, 0.4)$ and $\mu = (1, 0.5)$. Remark that in the right figure the scale is logarithmic.

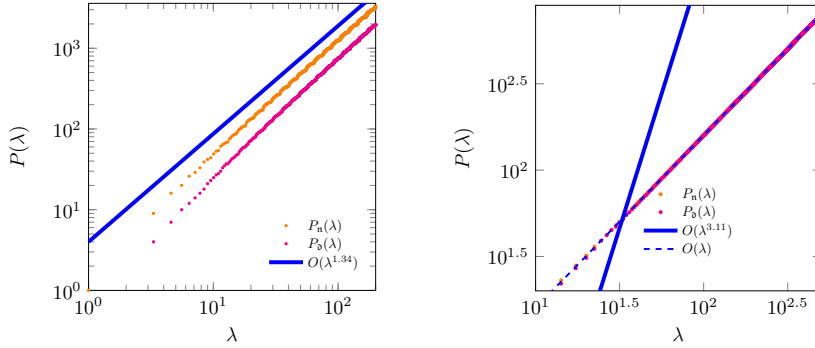


FIGURE 3. Comparison of $P_a(\lambda)$, $a \in \{\partial, n\}$, and the bounds of Theorem 4.1 and Proposition 4.4 for different values of α . Left: $\alpha = (0.45, 0.73)$, $\mu = (0.5, 0.5)$. Right: $\alpha = (0.8, 0.8)$, $\mu = (0.4, 0.6)$. In this latter case on the plot scale the difference between P_∂ and P_n is almost invisible.

Case 1 of Theorem 4.1: $d_s < 1$. We take $\alpha = (0.5, 0.2)$, $\mu = (1, 2)$, cf. Figure 2, left. The numerical results confirm the bounds of Theorem 4.1, Proposition 4.4: $P(\lambda) = O(\lambda)$.

Case 2 of Theorem 4.1: $d_s = 1$. The numerical experiment for the case $\alpha = (0.4, 0.6)$, $\mu = (0.5, 0.3)$, cf. Figure 2, right, indicates that the upper bound is sharp in this case: $P_a(\lambda) = O(\lambda \log \lambda)$.

Case 3 of Theorem 4.1: $d_s > 1$. We study two cases:

- $\alpha = (0.45, 0.73)$, $\mu = (0.5, 0.5)$, $d_s \approx 1.34$. See Figure 3, left.
- $\alpha = (0.8, 0.8)$, $\mu = (0.4, 0.6)$, $d_s \approx 3.11$. See Figure 3, right.

In the first case we see that the upper bound of Theorem 4.1 seems to be sharp, i.e. $P_{\mathbf{a}}(\lambda) = O(\lambda^{d_s})$. In the second case we observe a clear discrepancy between the upper bound provided by Theorem 4.1 and the actual behaviour of $P_{\mathbf{a}}(\lambda)$, which is close to the lower bound (i.e. $O(\lambda)$), cf. Proposition 4.4. The reason for this is that $\alpha_0 = \alpha_1$ (i.e. the tree is 'symmetric'); a theoretical justification can be found in [8].

Let us finally remark that in the experiment with $\boldsymbol{\alpha} = (0.45, 0.73)$, on the interval $(0, 200)$ we computed more than 3200 poles for the Neumann problem.

Conclusions. Numerical experiments suggest that when $\langle \boldsymbol{\alpha} \rangle \geq 1$ and when the tree \mathcal{T} is not symmetric (i.e. $\alpha_i \neq \alpha_j$, for $i \neq j$), the upper bound of Theorem 4.1 is sharp. This can fail in the presence of symmetries. Therefore, we expect the case $d_s > 1$ to be more difficult for the numerical treatment than the case $d_s < 1$ (this will be explained in more detail in the beginning of Section 5.1). In particular, in this case the number of poles on intervals of a fixed length $(a, a + \ell)$ increases as $a \rightarrow +\infty$. To see this, suppose that $P_{\mathbf{a}}(\lambda) = C_{\mathbf{a}}\lambda^{d_s} + o(\lambda^{d_s})$, with $C_{\mathbf{a}} > 0$, and assume that the number of poles on $(a, a + \ell)$ is bounded by a constant $M > 0$ for all $a > 0$. This would imply that on the interval $(0, n\ell)$, there are at most nM poles, and thus $P_{\mathbf{a}}(n\ell) = O(n)$ as $n \rightarrow +\infty$. However, by assumption, $P_{\mathbf{a}}(n\ell) = C_{\mathbf{a}}(n\ell)^{d_s} + o(n^{d_s})$, with $d_s > 1$, and thus we arrive at the contradiction.

5. Numerical resolution of (3.17). Numerical experiments. In this section we address the numerical aspects of the resolution of (3.17):

- in Section 5.1 we outline one strategy to compute $\Omega_{\mathbf{a},k}$ and $A_{\mathbf{a},k}$;
- in Section 5.2, we present a stable discretization of (3.17);
- Section 5.3 is dedicated to the numerical experiments.

5.1. Computing poles and zeros in the approximation $\Lambda_{\mathbf{a}}^N$. In order to use the approximation (3.15), (3.12), it is necessary to be able to evaluate $\Omega_{\mathbf{a},k}$, the poles of $\Lambda_{\mathbf{a}}$, and the respective (scaled) residues $A_{\mathbf{a},k}$. Because $\Lambda_{\mathbf{a}}(\omega)$ can be efficiently evaluated for each $\omega \in \mathbb{C}^+$ using the method described in [6] (and for $\omega \in \mathbb{C}^-$, we have $\Lambda_{\mathbf{a}}(\omega) = (\Lambda_{\mathbf{a}}(\omega^*))^*$), it would be rather natural to use classical contour integration techniques for computing the poles and the residues of $\Lambda_{\mathbf{a}}$. However,

- the location of poles is not known. This is aggravated by the fact that the poles and the zeros of $\Lambda_{\mathbf{a}}$ interlace (this can be proven rigorously), and thus a straightforward use of the argument principle does not seem to be possible.
- poles of $\Lambda_{\mathbf{a}}$ can be located very close to each other (which poses difficulties in choosing an integration contour for computing residues), see Section 4.2.2.
- evaluating $\Lambda_{\mathbf{a}}$ close to the real axis may be inaccurate, because of the proximity to the poles, cf. the error estimates in [6]. Let us remark that in practice we found this much less of a problem than the two previous issues.

To overcome (at least some of) these difficulties, we suggest to use an alternative strategy described in the sections that follow.

5.1.1. An auxiliary function. Let us introduce an auxiliary function (which, since $\Lambda_{\mathbf{a}}(\omega)$ is the symbol of the DtN, can be viewed as a Robin-to-Robin operator):

$$(5.1) \quad \mathbf{g}_{\mathbf{a}}(\omega) := (-\omega^{-1}\Lambda_{\mathbf{a}}(\omega) - i) (-\omega^{-1}\Lambda_{\mathbf{a}}(\omega) + i)^{-1}.$$

The following proposition relates the location of poles of $\Lambda_{\mathbf{a}}$ to the points ω where $\text{Re } \mathbf{g}_{\mathbf{a}}(\omega) = 0$ and the values of coefficients $A_{\mathbf{a},k}$ to the derivatives of $\mathbf{g}_{\mathbf{a}}$ in these points.

PROPOSITION 5.1. *The function $\mathbf{g}_{\mathbf{a}}$ is meromorphic in \mathbb{C} . Moreover,*

- (1) *if ω_0 is a pole of $\mathbf{g}_{\mathbf{a}}$, then $\text{Im } \omega_0 < 0$;*

- (2) $|\mathbf{g}_\alpha(\omega)| = 1$ when $\omega \in \mathbb{R}$;
(3) let $\omega_0 \in \mathbb{R}$. Then $\mathbf{g}_\alpha(\omega_0) = 1$ if and only if ω_0 is a pole of $\Lambda_\alpha(\omega)$.
(4) the coefficient $A_{\alpha,\ell}$, cf. (3.6), is given by $A_{\alpha,\ell} = 4i(\mathbf{g}'_\alpha(\Omega_{\alpha,\ell}))^{-1}$.

Proof. The function \mathbf{g}_α is meromorphic because Λ_α is such, cf. Theorem 3.2.

Proof of (2). (2) follows from the property $\omega^{-1}\Lambda_\alpha(\omega) \in \mathbb{R}$ for $\omega \in \mathbb{R}$, cf. (3.6).

Proof of (3). We prove \implies , while the other implication is immediate. Let $\mathbf{g}_\alpha(\omega_0) = 1$. Assume that ω_0 is not a pole of $\omega^{-1}\Lambda_\alpha(\omega)$. We have $\omega_0^{-1}\Lambda_\alpha(\omega_0) \in \mathbb{R}$; set $z = -\omega_0^{-1}\Lambda_\alpha(\omega_0) + i$. Then $\text{Im } z = 1$, but $\mathbf{g}_\alpha(\omega_0) = z^*z^{-1} = 1$, which implies that $\text{Im } z = 0$, thus a contradiction.

Proof of (1). By (2), $\mathbf{g}_\alpha(\omega)$ has no poles on \mathbb{R} , it thus remains to show that it has no poles in \mathbb{C}^+ . Because, by Corollary 3.4, $\omega \mapsto \omega^{-1}\Lambda_\alpha(\omega)$ is analytic in \mathbb{C}^+ , \mathbf{g}_α may have a poles in $\omega_0 \in \mathbb{C}^+$ if and only if $\omega_0^{-1}\Lambda_\alpha(\omega_0) = i$. This is impossible by Theorem 5.9 in [9]: for all $\omega \in \mathbb{C}^+$, we have $\text{Im}(\omega^{-1}\Lambda_\alpha(\omega)) < 0$.

Proof of (4). In the vicinity of the pole $\Omega_{\alpha,\ell}$ it holds that

$$\begin{aligned} \omega^{-1}\Lambda_\alpha(\omega) &= -\frac{A_{\alpha,\ell}\omega}{\Omega_{\alpha,\ell}^2 - \omega^2} + O(1), \text{ and} \\ (\omega^{-1}\Lambda_\alpha(\omega))' &= -\frac{2A_{\alpha,\ell}\Omega_{\alpha,\ell}^2}{(\omega^2 - \Omega_{\alpha,\ell}^2)^2} + O((\omega^2 - \Omega_{\alpha,\ell}^2)^{-1}). \end{aligned}$$

Inserting the above into

$$\mathbf{g}'_\alpha(\omega) = -\frac{2i(\omega^{-1}\Lambda_\alpha(\omega))'}{(-\omega^{-1}\Lambda_\alpha(\omega) + i)^2},$$

we deduce that $\lim_{\omega \rightarrow \Omega_{\alpha,\ell}} \mathbf{g}'_\alpha(\omega) = 4iA_{\alpha,\ell}^{-1}$. \square

One draws two important conclusions from Proposition 5.1:

- to find the poles of Λ_α it suffices to find $\omega \in \mathbb{R}_*$ s.t. $\mathbf{g}_\alpha(\omega) = 1$.
- to compute $A_{\alpha,\ell}$ it suffices to compute $\mathbf{g}'_\alpha(\Omega_{\alpha,\ell})$.

All of the above requires a method for evaluation of \mathbf{g}_α on the real axis. For computing \mathbf{g}_α we will use the same ideas as in [6] for evaluating Λ_α in \mathbb{C}^+ . We start by writing a non-linear equation satisfied by \mathbf{g}_α .

5.1.2. \mathbf{g}_α as a solution of a non-linear equation. An equation for \mathbf{g}_α can be obtained from the equation for Λ_α in [9].

LEMMA 5.2 (Lemmas 5.3, 5.5 in [9]). *The symbol of the reference DtN operator $\Lambda = \Lambda_\alpha$, $\alpha \in \{\mathfrak{n}, \mathfrak{d}\}$, is a unique even solution of the problem: find $\Lambda : \mathbb{C} \rightarrow \mathbb{C}$, s.t.*

$$(5.2) \quad \Lambda(\omega) = -\omega \frac{\omega \tan \omega - \mathbf{F}_{\alpha,\mu}(\omega)}{\tan \omega \mathbf{F}_{\alpha,\mu}(\omega) + \omega}, \quad \mathbf{F}_{\alpha,\mu}(\omega) = \sum_{i=0}^{p-1} \frac{\mu_i}{\alpha_i} \Lambda(\alpha_i \omega),$$

that is analytic in the origin, and whose value $\Lambda(0)$ is specified by Proposition 3.3.

The above equation allows to obtain an equation similar to (5.2) satisfied by \mathbf{g}_α . For this we 1) re-express Λ_α via \mathbf{g}_α from (5.1); 2) replace $\Lambda_\alpha(\alpha_j \omega)$ in the right-hand side of (5.2) by the obtained expression; 3) substitute the obtained expression for $\Lambda_\alpha(\omega)$ into the right hand side of (5.1). This procedure yields

$$(5.3) \quad \mathbf{g}_\alpha(\omega) = -e^{2i\omega} \frac{1 - \mathbf{g}_{\alpha,\mu}(\omega)}{1 + \mathbf{g}_{\alpha,\mu}(\omega)}, \quad \mathbf{g}_{\alpha,\mu}(\omega) = \sum_{j=0}^{p-1} \mu_j \frac{1 + \mathbf{g}_\alpha(\alpha_j \omega)}{1 - \mathbf{g}_\alpha(\alpha_j \omega)}.$$

Using the connection between (5.2) and (5.3) it is easy to obtain the following result.

LEMMA 5.3. *The function $\mathbf{g}_\mathbf{a}$, $\mathbf{a} \in \{\mathfrak{d}, \mathfrak{n}\}$ is a unique even meromorphic solution of the equation (5.3) that is analytic in the origin, satisfies $\mathbf{g}_\mathbf{a}(\omega)\mathbf{g}_\mathbf{a}(-\omega) = 1$ for all $\omega \in \mathbb{C}$, as well as the following condition in the origin:*

- when $\langle \mu/\alpha \rangle \leq 1$, $\mathbf{g}_\mathfrak{d}(0) = \mathbf{g}_\mathfrak{n}(0) = -1$.
- when $\langle \mu\alpha \rangle < 1 < \langle \mu/\alpha \rangle$, $\mathbf{g}_\mathfrak{n}(0) = -1$ and $\mathbf{g}_\mathfrak{d}(0) = 1$;
- when $\langle \mu\alpha \rangle \geq 1$, $\mathbf{g}_\mathfrak{d}(0) = \mathbf{g}_\mathfrak{n}(0) = 1$.

Proof. The proof is left to the reader. Remark that the condition $\mathbf{g}_\mathbf{a}(\omega)\mathbf{g}_\mathbf{a}(-\omega) = 1$ corresponds to the evenness of $\Lambda_\mathbf{a}$. \square

REMARK 5.4. *Because we are interested in calculating $\mathbf{g}_\mathbf{a}$ on the real axis based on (5.3), it is important to check whether (5.3) is well-defined for all $\omega \in \mathbb{R}$.*

First, let us remark that if $\lim_{\omega \rightarrow \omega_0} \mathbf{g}_{\alpha, \mu}(\omega) = \infty$, $\mathbf{g}_\mathbf{a}(\omega_0)$ is well-defined: $\mathbf{g}_\mathbf{a}(\omega_0) = e^{2i\omega_0}$.

It is possible to prove that $\lim_{\omega \rightarrow \omega_0} \mathbf{g}_{\alpha, \mu}(\omega) = \infty$ if and only if, for some ℓ , $\mathbf{g}_\mathbf{a}(\alpha_\ell \omega_0) = 1$.

Second, we remark that the denominator of (5.3) cannot vanish: otherwise this would have implied that in such points ω , $\mathbf{g}_\mathbf{a}(\omega) = \infty$ which contradicts Proposition 5.1 (1) and the uniqueness Lemma 5.3. We thus rewrite (5.3) for $\omega \in \mathbb{R}$ as follows:

$$(5.4) \quad \mathbf{g}_\mathbf{a}(\omega) = e^{2i\omega} \begin{cases} \frac{\mathbf{g}_{\alpha, \mu}(\omega) - 1}{\mathbf{g}_{\alpha, \mu}(\omega) + 1}, & \text{if } \mathbf{g}_\mathbf{a}(\alpha_j \omega) \neq 1, \quad \forall j, \\ 1, & \text{otherwise.} \end{cases}$$

5.1.3. A method for calculating $\mathbf{g}_\mathbf{a}$ in a point $\omega \in \mathbb{R}$. Let us discuss how to compute $\mathbf{g}_\mathbf{a}(\omega)$ in a point $\omega \in \mathbb{R}$. We consider two cases: $|\omega| < r$ and $|\omega| \geq r$, for a fixed small enough r .

Description of the method.

Case $|\omega| < r$. By Proposition 5.1, $\mathbf{g}_\mathbf{a}$ is analytic in the vicinity of the origin. Thus it can be approximated using the truncated Taylor expansion:

$$(5.5) \quad \mathbf{g}_\mathbf{a}(\omega) \approx \mathbf{g}_\mathbf{a}^{N_*}(\omega) := \sum_{n=0}^{N_*} \omega^n g_{\mathbf{a}, n}, \quad \text{for a fixed } N_* > 0,$$

where $g_{\mathbf{a}, n}$, $n \in \mathbb{N}$, are the Taylor coefficients of $\mathbf{g}_\mathbf{a}$ in $\omega = 0$. They can be found by power matching from (5.1) and the known recursive expressions for the Taylor coefficients of $\Lambda_\mathbf{a}$ in the origin given in [9].

Case $|\omega| \geq r$. The expression (5.4) shows that, provided $\omega \in \mathbb{R}$, knowing $\mathbf{g}_\mathbf{a}(z)$ for $|z| < |\alpha|_\infty |\omega|$ (recall that $|\alpha|_\infty < 1$) allows to compute $\mathbf{g}_\mathbf{a}(\omega)$. In this sense, the equation (5.4) resembles (5.2). Hence for computing $\mathbf{g}_\mathbf{a}(\omega)$, we can employ the same method as for computing $\Lambda_\mathbf{a}(\omega)$ in [6]. We will not present it here, as it is lengthy and its application to evaluating $\mathbf{g}_\mathbf{a}$ is straightforward. It is based on the two ideas:

1. To compute $\mathbf{g}_\mathbf{a}(\omega)$, by (5.4), it suffices to compute $\mathbf{g}_\mathbf{a}(\alpha_j \omega)$, for $j = 0, \dots, p-1$, and next use (5.4). Remark that $|\alpha_j \omega| \leq |\alpha|_\infty |\omega| < |\omega|$. The same reasoning can be applied to each of $\mathbf{g}_\mathbf{a}(\alpha_j \omega)$, $j = 0, \dots, p-1$.

Further application of this idea allows to reduce the question of evaluation of $\mathbf{g}_\mathbf{a}(\omega)$ to the question of computing

$$\mathbf{g}_\mathbf{a}(\alpha_{i_1} \cdots \alpha_{i_L} \omega), \quad i_1, \dots, i_L \in \{0, \dots, p-1\},$$

where L is such that $|\alpha|_\infty^L |\omega| < r$. With such L , $|\alpha_{i_1} \cdots \alpha_{i_L} \omega| \leq |\alpha|_\infty^L |\omega| < r$.

2. the values $\mathbf{g}_a(\alpha_{i_1} \cdots \alpha_{i_L} \omega)$ are then evaluated using (5.5):

$$(5.6) \quad \mathbf{g}_a(\alpha_{i_1} \cdots \alpha_{i_L} \omega) \approx \mathbf{g}_a^{N_*}(\alpha_{i_1} \cdots \alpha_{i_L} \omega).$$

Preservation of the property $|\mathbf{g}_a(\omega)| = 1$. As seen from the above, the method of [6] is based on a repeated application of (5.4); let us prove that it preserves the property $|\mathbf{g}_a(\omega)| = 1$.

PROPOSITION 5.5. *Let $\omega \in \mathbb{R}_*$ be fixed. Let $(g_j)_{j=0}^{p-1} \in \mathbb{C}^p$ be s.t. $|g_j| = 1$ for all $0 \leq j \leq p-1$. Then $g \in \mathbb{C}$ given by*

$$(5.7) \quad g = e^{2i\omega} \begin{cases} \frac{g_{\alpha,\mu}(\omega)-1}{g_{\alpha,\mu}(\omega)+1}, & \text{if } \forall j, g_j \neq 1, \\ 1, & \text{otherwise,} \end{cases} \quad g_{\alpha,\mu} = \sum_{j=0}^{p-1} \mu_j \frac{1+g_j}{1-g_j},$$

satisfies $|g| = 1$.

Proof. The result being obvious if for some j $g_j = 1$, let us prove it in the opposite case. A simple computation yields

$$|g|^2 = \frac{(1 - \operatorname{Re} g_{\alpha,\mu})^2 + (\operatorname{Im} g_{\alpha,\mu})^2}{(1 + \operatorname{Re} g_{\alpha,\mu})^2 + (\operatorname{Im} g_{\alpha,\mu})^2}.$$

It remains to show that $\operatorname{Re} g_{\alpha,\mu} = 0$. This follows by a direct computation:

$$\operatorname{Re} g_{\alpha,\mu} = \sum_{j=0}^{p-1} \mu_j \frac{1 - |g_j|^2}{|1 - g_j|^2} = 0, \text{ since } |g_j| = 1 \text{ for all } j. \quad \square$$

Assume that for all i_1, \dots, i_L , it holds that $|\mathbf{g}_a^{N_*}(\alpha_{i_1} \cdots \alpha_{i_L} \omega)| = 1$ (cf. (5.6)). Since the approximation of \mathbf{g}_a , namely $\tilde{\mathbf{g}}_a$, is computed by a repeated application of (5.4), according to the above lemma, it holds that $|\tilde{\mathbf{g}}_a(\omega)| = 1$.

REMARK 5.6. *For the moment we have only numerical evidence of convergence of the method, as well as of its stability when $|\mathbf{g}_a^{N_*}(\alpha_{i_1} \cdots \alpha_{i_L} \omega)| = 1 \pm \varepsilon$, for ε small.*

Complexity. From the results of [6], it follows that for a fixed $r > 0$, $N_* \in \mathbb{N}$, the asymptotic complexity (as $|\omega| \rightarrow +\infty$) of the method scales as $O(\log^{p+1} |\omega|)$.

5.1.4. Computing poles and residues of Λ_a . Computation of the poles of Λ_a and the coefficients $A_{a,\ell}$ is based on the results of Proposition 5.1. Let us show how to compute the poles of Λ_a on the interval $(0, L)$. First we subdivide $(0, L)$ into small intervals and interpolate \mathbf{g}_a on each of these intervals using the Chebyshev interpolation. The resulting piecewise-Chebyshev interpolant is denoted by $\mathbf{g}_{a,c}$.

We next find the poles according to Proposition 5.1 (3). The Chebyshev interpolants do not preserve the property $|\mathbf{g}_a(\omega)| = 1$, and therefore, instead of finding the points where $\operatorname{Re} \mathbf{g}_{a,c}(\omega) = 1$, we

- 1) compute zeros z_k of the polynomial interpolant $\operatorname{Im} \mathbf{g}_{a,c}(\omega)$ (by Proposition 5.1 (2), if $\operatorname{Im} \mathbf{g}_a(\omega) = 0$, then $\operatorname{Re} \mathbf{g}_a(\omega) = \pm 1$);
- 2) check whether $\operatorname{Re} \mathbf{g}_{a,c}(z_k) > c > 0$. If this is the case, we consider that z_k is an approximation to the pole of Λ_a .

The coefficients $A_{a,k}$ are evaluated by computing $\mathbf{g}'_{a,c}(z_k)$, cf. Proposition 5.1(4).

REMARK 5.7. *The reason why we subdivide the original interval $(0, L)$ into multiple sub-intervals and interpolate \mathbf{g}_a on the sub-intervals is the following: despite the fact that \mathbf{g}_a is smooth, it may oscillate rapidly (depending on the values α, μ), and hence require a high degree polynomial interpolant. This is illustrated in Figure 4.*

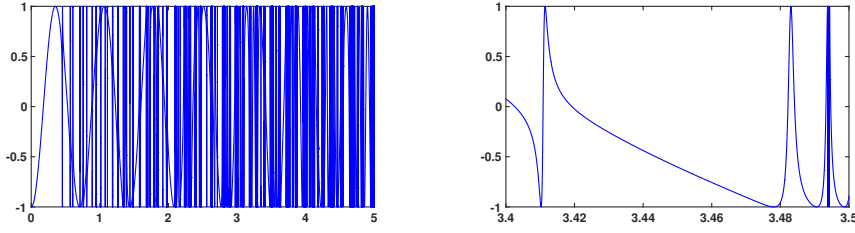


FIGURE 4. *Left: dependence of $\text{Re } \mathbf{g}_n(\omega)$ on ω ; $\boldsymbol{\alpha} = (0.8, 0.75)$ and $\boldsymbol{\mu} = (0.5, 0.5)$. Right: the close-up for the interval $(3.4, 3.5)$. In this case $\boldsymbol{\Lambda}_n$ has about 1100 poles on $(0, 5)$.*

The implementation of this algorithm was done using the Chebfun [3, 19], which allows to construct a highly accurate approximation of $\mathbf{g}_{\mathbf{a},c}$ and contains an automated procedure for choosing the degree of the interpolant, see [2, 19]. If the Chebfun fails to construct an accurate interpolant, we further subdivide the interpolation interval.

REMARK 5.8. *As remarked above, the Chebyshev interpolants do not preserve the property $|\mathbf{g}_{\mathbf{a}}(\omega)| = 1$, but this does not seem to pose significant problems in practice.*

5.2. Discretization. In this section we discuss the discretization of (3.17), starting with the semi-discretization in space, and then show a discretization in time. Next, we discuss its stability and convergence. All over this section we fix m and N . In the definition of the discretized quantities, we will omit the indices N, m, \mathbf{a} .

5.2.1. Semi-discretization in space. Let $U_h \subset \mathbf{V}_{\boldsymbol{\mu}}(\mathcal{T}^m)$ be an extension of the Lagrange \mathbb{P}_1 space to the case of fractal trees, defined like in [6]. By $\mathbf{u}(t) \in \mathbb{R}^{N_s}$ we denote the respective vector of the degrees of freedom (nodal values) that approximates $u_m^{N,\mathbf{a}}(t)$, and by $\boldsymbol{\lambda}_{n,k}^h(t) \in \mathbb{R}^{p^m}$ an approximation of $\boldsymbol{\lambda}_{n,k}(t) \in \mathbb{R}^{p^m}$. The mass and stiffness matrices are denoted by \mathbf{M} and \mathbf{K} (remark that they are constructed with respect to the weighted $L_{\boldsymbol{\mu}}^2(\mathcal{T})$ product). Let also the matrix \mathbf{P} be defined as $\mathbf{P}_{j\ell} = \varphi_{\ell}(M_{m,j})$.

Formulation. The discretization in space of (3.17) in the algebraic form reads: find $\mathbf{u} \in C^1(\mathbb{R}^+; \mathbb{R}^{N_s})$, s.t. $\mathbf{u}(0) = \partial_t \mathbf{u}(0) = 0$ and

$$\begin{aligned}
 & \mathbf{M} \partial_t^2 \mathbf{u} + \mathbf{K} \mathbf{u} + \mathbf{P}^T \mathbf{W}_m \mathbf{D}_m \langle \boldsymbol{\mu} / \boldsymbol{\alpha} \rangle \boldsymbol{\Lambda}_{\mathbf{a}}(0) \mathbf{P} \mathbf{u} \\
 (5.8) \quad & + \mathbf{P}^T \mathbf{W}_m \mathbf{D}_m \sum_{k=0}^{p-1} \sum_{i=0}^{N-1} A_{\mathbf{a},i} \frac{\mu_k}{\alpha_k} \partial_t \boldsymbol{\lambda}_{i,k}^h = \mathbf{M} \mathbf{f}^n, \\
 & \partial_t^2 \boldsymbol{\lambda}_{i,k}^h + \alpha_k^{-1} \Omega_{\mathbf{a},i}^2 \mathbf{D}_m^2 \boldsymbol{\lambda}_{i,k}^h = \mathbf{P} \mathbf{u}, \quad \boldsymbol{\lambda}_{i,k}^h(0) = \partial_t \boldsymbol{\lambda}_{i,k}^h(0) = 0.
 \end{aligned}$$

5.2.2. Discretization in Time. Let us describe how we discretize in time the approximate problem (5.8). To obtain a stable discretization, the main idea is to use the explicit **leapfrog** discretization for the volumic terms, and the implicit **trapezoid rule** discretization of the boundary terms. First, however, we introduce some notation. Provided a time step Δt , let v^n be an approximation to $v(\cdot, n\Delta t)$. Let

$$\begin{aligned}
 D_{\Delta t} v^n &= \frac{v^{n+1} - v^{n-1}}{2\Delta t}, \quad D_{\Delta t}^2 v^n = \frac{v^{n+1} - 2v^n + v^{n-1}}{(\Delta t)^2}, \quad D_{\Delta t} v^{n+\frac{1}{2}} = \frac{v^{n+1} - v^n}{\Delta t}, \\
 \{v^n\}_{1/4} &= \frac{v^{n+1} + 2v^n + v^{n-1}}{4}, \quad v^{n+1/2} = \frac{v^n + v^{n+1}}{2}.
 \end{aligned}$$

Formulation. For simplicity we will assume that the source term f in (3.17) satisfies $f \in C^1(\mathbb{R}^+; L_\mu^2(\mathcal{T}^n))$, $f(0) = \frac{d}{dt}f(0) = 0$. The discretization of (3.17a) reads: given $\mathbf{u}^0 = 0$, $\mathbf{u}^1 = 0 \in \mathbb{R}^{N_s}$, find $(\mathbf{u}^n)_{n \in \mathbb{N}} \subset \mathbb{R}^{N_s}$, s.t.

$$(5.9a) \quad \begin{aligned} & \mathbf{M}D_{\Delta t}^2 \mathbf{u}^n + \mathbf{K}\mathbf{u}_N^n + \mathbf{P}^T \langle \boldsymbol{\mu} / \boldsymbol{\alpha} \rangle \boldsymbol{\Lambda}_a(0) \mathbf{W}_m \mathbf{D}_m \mathbf{P} \{ \mathbf{u}^n \}_{1/4} \\ & + \mathbf{P}^T \mathbf{W}_m \mathbf{D}_m \sum_{k=0}^{p-1} \sum_{i=1}^N A_{\alpha,i} \frac{\mu_k}{\alpha_k} D_{\Delta t} (\boldsymbol{\lambda}_{i,k}^h)^n = \mathbf{M}\mathbf{f}^n, \end{aligned}$$

$$(5.9b) \quad D_{\Delta t}^2 (\boldsymbol{\lambda}_{i,k}^h)^n + \alpha_k^{-1} \Omega_{\alpha,i}^2 \mathbf{D}_m^2 \left\{ (\boldsymbol{\lambda}_{i,k}^h)^n \right\}_{1/4} = D_{\Delta t} \mathbf{P}\mathbf{u}^n,$$

$$(5.9c) \quad (\boldsymbol{\lambda}_{i,k}^h)^0 = (\boldsymbol{\lambda}_{i,k}^h)^1 = 0.$$

Stability. The formulation (5.9a-5.9c) is stable under the CFL condition

$$(5.10) \quad C_{CFL} = \left(\frac{\Delta t}{2} \right)^2 \rho(\mathbf{M}^{-1/2} \mathbf{K} \mathbf{M}^{-1/2})^{-1} < 1,$$

where $\rho(A)$ is the spectral radius of a matrix A . To see this, let us first introduce the notation: $\langle \mathbf{v}, \mathbf{q} \rangle_A = \langle \mathbf{A}\mathbf{v}, \mathbf{q} \rangle$, $\|\mathbf{v}\|_A^2 = \langle \mathbf{v}, \mathbf{v} \rangle_A$. Let us define

$$\begin{aligned} \mathbb{E}^{n+1/2} &= \frac{1}{2} \left(\left\| D_{\Delta t} \mathbf{u}^{n+1/2} \right\|_{\mathbf{M}}^2 - \left(\frac{\Delta t}{2} \right)^2 \left\| D_{\Delta t} \mathbf{u}^{n+1/2} \right\|_{\mathbf{K}}^2 \right) + \frac{1}{2} \left\| \mathbf{u}^{n+1/2} \right\|_{\mathbf{K}}^2 \\ &+ \frac{1}{2} \langle \boldsymbol{\mu} / \boldsymbol{\alpha} \rangle \boldsymbol{\Lambda}_a(0) \left\| \mathbf{P}\mathbf{u}^{n+1/2} \right\|_{\mathbf{W}_m \mathbf{D}_m}^2 + \sum_{i=1}^N A_{\alpha,i} \sum_{k=0}^{p-1} \frac{\mu_k}{\alpha_k} \mathbb{E}_{i,k}^{n+1/2}, \\ \mathbb{E}_{i,k}^{n+1/2} &= \frac{1}{2} \left\| D_{\Delta t} (\boldsymbol{\lambda}_{i,k}^h)^{n+1/2} \right\|_{\mathbf{W}_m \mathbf{D}_m}^2 + \frac{\alpha_k^{-1} \Omega_{\alpha,i}^2}{2} \left\| \mathbf{D}_m (\boldsymbol{\lambda}_{i,k}^h)^{n+1/2} \right\|_{\mathbf{W}_m \mathbf{D}_m}^2. \end{aligned}$$

The condition (5.10) ensures that $\mathbb{E}^{n+1/2} \geq 0$.

THEOREM 5.9 (Stability of (5.9)). *Let $(\mathbf{u}^n)_{n \in \mathbb{N}}$ solve (5.9), and let (5.10) hold true. Then, with $C > 0$ depending on $\boldsymbol{\alpha}, \boldsymbol{\mu}$ and the problem (Dirichlet or Neumann),*

$$\sqrt{\mathbb{E}^{n+1/2}} \leq C \Delta t \sum_{k=0}^n \|\mathbf{f}^k\|_{\mathbf{M}}, \quad n \in \mathbb{N}.$$

Proof. The result is obtained by testing the equation (5.9a) with $D_{\Delta t} \mathbf{u}^n$. The only 'non-classical' terms are related to $\boldsymbol{\lambda}$, and can be handled using (5.9b):

$$\begin{aligned} & \left(\mathbf{W}_m \mathbf{D}_m D_{\Delta t} (\boldsymbol{\lambda}_{i,k}^h)^n, D_{\Delta t} \mathbf{P}\mathbf{u}^n \right) = \left(\mathbf{W}_m \mathbf{D}_m D_{\Delta t} (\boldsymbol{\lambda}_{i,k}^h)^n, D_{\Delta t}^2 (\boldsymbol{\lambda}_{i,k}^h)^n \right) \\ & + \left(\mathbf{W}_m \mathbf{D}_m D_{\Delta t} (\boldsymbol{\lambda}_{i,k}^h)^n, \alpha_k^{-1} \Omega_{\alpha,i}^2 \mathbf{D}_m^2 \left\{ (\boldsymbol{\lambda}_{i,k}^h)^n \right\}_{1/4} \right). \end{aligned}$$

The above yields :

$$\mathbb{E}^{n+1/2} - \mathbb{E}^{n-1/2} = \Delta t \left\langle \mathbf{f}^n, \frac{\mathbf{u}^{n+1} - \mathbf{u}^{n-1}}{\Delta t} \right\rangle_{\mathbf{M}},$$

which can be bounded using a discrete Gronwall inequality, see [7, Appendix E].

REMARK 5.10. *As discussed in [6], the CFL condition (5.10) coincides with the CFL condition for a \mathbb{P}_1 -discretization of a non-weighted wave equation (since the weights are piecewise-constant, and $u_m^{\alpha,N}$ satisfies (2.2) on each branch). Moreover, in our case the CFL condition is not affected by the DtN approximation, because the related terms are discretized with the implicit trapezoid rule.*

5.2.3. Remarks on convergence. Like for the CQ discretization in [6], it is not difficult to demonstrate that (5.9) is of second order in time and first order in space, when measuring the error in the energy norm, with the constants depending on the computational time T polynomially and on some $W^{\ell,1}(0, T; L^2_\mu(\mathcal{T}^m))$ -norm of f . The convergence estimates can be shown to be independent of N . As the proof is classical, we will not state the respective result here.

5.3. Numerical Results. All the experiments of this section are performed on the reference tree. Moreover, we use the scheme (5.9a-5.9c) with the mass-lumped finite elements (and all the norms are computed using mass-lumped matrices). All over this section, we will omit the indices m and \mathbf{a} .

5.3.1. Validity of the method. To validate the correctness of the approach, we compare it to a highly accurate convolution quadrature approximation of the transparent boundary conditions, cf. [6]. In particular, we truncate the tree to 3 generations, and compute the solution on the tree \mathcal{T}^m , $m = 2$, with the help of the N -term transparent boundary conditions. The reference solution u_{ref} is computed on the truncated tree \mathcal{T}^{m+1} (i.e. the tree with 4 generations), with the help of the convolution quadrature method, with the same discretization parameters. In all the cases we choose the discretization with $h = 10^{-4}$ and $\Delta t \approx 9.9 \cdot 10^{-5}$. In what follows we will denote by u_N^n (resp. u_{ref}^n) the solution to (5.9) at the time step n . We

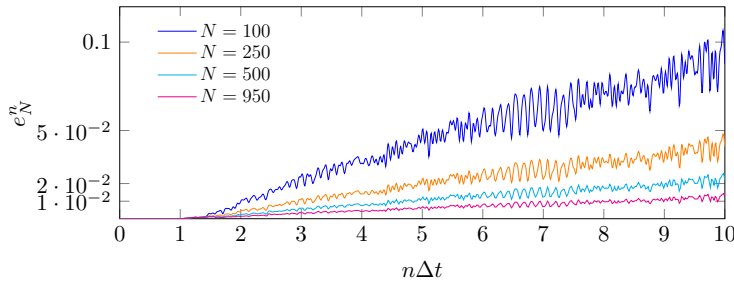


FIGURE 5. Dependence of the error e_N^n defined in (5.12) on time $n\Delta t$ for different values of the truncation parameter N .

solve the Dirichlet problem for $\boldsymbol{\alpha} = (0.3, 0.6)$, $\boldsymbol{\mu} = (0.5, 1)$. As a source we take the function supported on the root edge of the tree

$$(5.11) \quad f(s, t) = 10^5 \exp(-\sigma(s - 0.5)^2 - \sigma(t - 0.5)^2)(s - 0.5), \quad \sigma = 10^3.$$

The above function is approximately band-limited in time with the maximal frequency in its Fourier transform being $\omega_{max} \approx 107$ (we cut-off at 10^{-5} -accuracy). This implies that the maximal frequency present in the Fourier transform of $\mathcal{B}_m^{\mathbf{a}} \gamma_m u$, cf. (2.12), is roughly $\omega_{max} |\boldsymbol{\alpha}|_\infty^{m+1} \approx 0.6^3 \cdot 107 \approx 23$. Thus, N should be chosen large enough to ensure that all the poles inside the interval $(0, 23)$ are included into the approximation (3.15), i.e. $N \geq 27$. A more precise error control is achieved by computing the value $r_N \equiv r_{\mathfrak{d}, N}$ as described in Section 4.1. In particular,

$$r_{100} \approx 9 \cdot 10^{-3}, \quad r_{250} \approx 4.1 \cdot 10^{-3}, \quad r_{500} \approx 2.2 \cdot 10^{-3}, \quad r_{950} \approx 1.2 \cdot 10^{-3}.$$

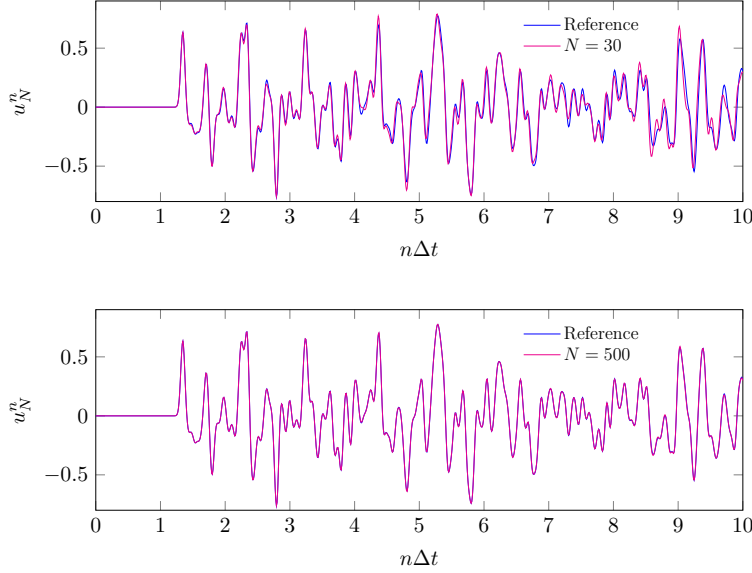


FIGURE 6. *Top: dependence of the solution u_N^n measured in the middle of the edge $\Sigma_{2,0}$ of the tree on time $n\Delta t$. Top: $N = 30$, bottom: $N = 500$*

The dependence of the solution u_N on time evaluated in one point of the tree is shown in Figure 6. We plot the dependence of the error

$$(5.12) \quad e_N^n = \frac{\|u_N^n - u_{ref}^n\|_{L_\mu^2(\mathcal{T}^{m-1})}}{\max_\ell \|u_{ref}^\ell\|_{L_\mu^2(\mathcal{T}^{m-1})}},$$

on time $n\Delta t$ for different values of N in Figure 5.

5.3.2. Convergence rates. In this section we study the convergence rates of the method, according to the results of Theorems 4.3, 3.9. We compare the quantity e_{rel}^N to the quantity $r_N \equiv r_{n,N}$, computed numerically as described in Section 4.1, as well as a theoretical upper bound given in Theorem 4.3. The results are given in Figures 7, 8. In these figures we observe in particular that the numerically computed value r_N provides an excellent estimate for the convergence rates, as expected, and can be potentially used as an error estimator. To verify the result of Theorem 4.3, we conduct four numerical experiments, which cover all three cases of Theorem 4.3. We compute the solution u_N to the Neumann problem on a truncated tree \mathcal{T}^m , with $m = 2$, with the help of the approximated transparent boundary conditions (3.15), for different values of N , and compare it to the reference solution u_{ref} computed with the help of the convolution quadrature method [6] on the truncated tree \mathcal{T}^m . In all the experiments we use the discretization with the spatial step $h = 10^{-4}$ and the time step $\Delta t = 9.9 \cdot 10^{-5}$. As a source term we take (5.11), with $\sigma = 10^2$, supported on the root edge of \mathcal{T}^m . All the computations are done on the time interval $(0, T)$, with $T = 10$, divided into N_t time steps. We measure the dependence of the following

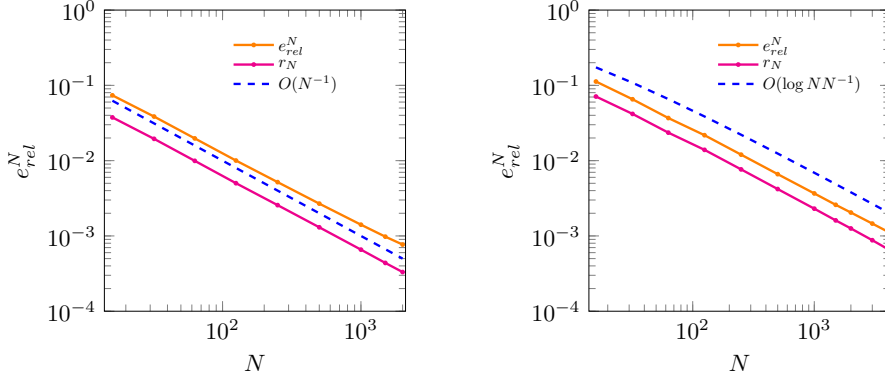


FIGURE 7. Relative error (5.13) depending on N . Left: $\alpha = (0.2, 0.5)$, $\mu = (0.6, 0.1)$ ($d_s < 1$, with $r_N \leq CN^{-1}$). Right: $\alpha = (0.7, 0.3)$, $\mu = (0.3, 0.6)$ ($d_s = 1$, with $r_N \leq CN^{-1} \log N$).

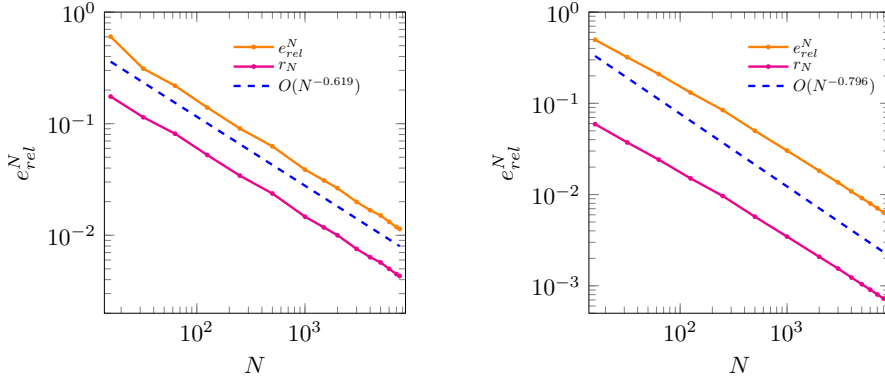


FIGURE 8. Relative error (5.13) depending on N . Left: $\alpha = (0.7, 0.6)$, $\mu = (0.3, 0.6)$ ($d_s \approx 1.615$, $r_N \leq CN^{-\frac{1}{d_s}}$). Right: $\alpha = (0.5, 0.65)$, $\mu = (2, 1)$ ($d_s \approx 1.256$, $r_N \leq CN^{-\frac{1}{d_s}}$). In this latter case the Dirichlet and Neumann problems coincide.

relative error on the order N of the transparent boundary conditions:

$$(5.13) \quad e_{rel}^N := \frac{e_{abs}^N}{\max_{\ell=0, \dots, N_t} \|u_{ref}^\ell\|_{L_\mu^2(\mathcal{T}^m)}}, \quad e_{abs}^N = \max_{\ell=0, \dots, N_t} \|u_N^\ell - u_{ref}^\ell\|_{L_\mu^2(\mathcal{T}^m)}.$$

As a complement to Figures 7, 8, we present the numerically estimated order of convergence associated to different experiments in Table 1. We observe a rather good agreement with the theoretical convergence estimates, especially in the cases $\alpha = (0.7, 0.3)$ and $\alpha = (0.7, 0.6)$. In the case $\alpha = (0.5, 0.65)$, where the numerically established convergence rates are somewhat different from the theoretical one, it appears that the numerical convergence rates are quite close to the ones measured from the values r_N . Most likely the discrepancy between the theoretical and the numerical rate is related to the fact that the asymptotic regime has not been reached for the range of N considered. Finally, in the case $\alpha = (0.2, 0.5)$, we remark that the con-

Value of N	Numerical convergence rate d			
	$\alpha = (0.2, 0.5)$	$\alpha = (0.7, 0.3)$	$\alpha = (0.7, 0.6)$	$\alpha = (0.5, 0.65)$
N_k				
16	-	-	-	-
32	0.94	1.15	0.95	0.63
63	0.99	1.15	0.52	0.63
125	0.99	0.99	0.66	0.68
250	0.95	1.1	0.62	0.64
500	0.95	1.0	0.53	0.75
1000	0.93	1.0	0.69	0.72
2000	0.88	0.98	0.56	0.73
4000	-	0.96	0.65	0.75
7000	-	-	0.62	0.76
Theoretical d	1	1	0.62	0.796

TABLE 1

Numerically measured convergence rates in different experiments. In the particular case of $\alpha = (0.7, 0.3)$ (where the convergence is $O(N^{-1} \log N)$), the quantity provided in the above table is defined

$$as \ d = \frac{\log\left(\frac{e_{rel}^{N_{k+1}}}{e_{rel}^{N_k}}\right)}{\log\left(\frac{N_{k+1}^{-1} \log N_{k+1}}{N_k^{-1} \log N_k}\right)}.$$

vergence order deteriorates slightly. Because there exists a discrepancy between the convergence rates measured from the numerical error and the ones measured for the numerically computed value r_N (where it is very close to 1), we think that either it is related to the accuracy of computation of the poles and residues in the method, or the discretization error becomes significant in this case.

6. Conclusions and Open Questions. In this work, we have constructed transparent boundary conditions for the weighted wave equation on a self-similar one-dimensional fractal tree. The approach presented here is alternative to the convolution quadrature [6] and is based on the truncation of the meromorphic series representing the symbol of the DtN operator. The complexity of the method depends on the number of poles in the truncated series; we have presented estimates on the number of poles, required to achieve a desired accuracy ε . While the convergence in term of the number of poles is rather slow, one of the advantages of this method is that its cost does not increase with time (unlike the convolution quadrature approach). Our future efforts are directed towards improving the convergence of the technique, based on approximation of the remainder of the meromorphic series.

Acknowledgements. We are grateful to Adrien Semin (TU Darmstadt, Germany) for providing his code NETWAVES.

REFERENCES

- [1] The Audible Human Project of acoustics and vibrations laboratory of University of Illinois at Chicago, 2007-2014.
- [2] Jared L. Aurentz and Lloyd N. Trefethen, Chopping a Chebyshev series, ACM Trans. Math. Software **43** (2017), no. 4, Art. 33, 21.
- [3] T. A Driscoll, N. Hale, and L. N. Trefethen, Chebfun guide, Pafnuty Publications, 2014.
- [4] Bjorn Engquist and Andrew Majda, Absorbing boundary conditions for the numerical simulation of waves, Math. Comp. **31** (1977), no. 139, 629–651.
- [5] Céline Grandmont, Bertrand Maury, and Nicolas Meunier, A viscoelastic model with non-local damping application to the human lungs, M2AN Math. Model. Numer. Anal. **40** (2006),

- no. 1, 201–224.
- [6] Patrick Joly and Maryna Kachanovska, Transparent boundary conditions for wave propagation in fractal trees: convolution quadrature approach, submitted, August 2019.
 - [7] ———, Transparent boundary conditions for wave propagation in fractal trees: convolution quadrature approach (extended report), <https://hal.archives-ouvertes.fr/hal-02265345>, August 2019.
 - [8] ———, Local transparent boundary conditions for wave propagation in fractal trees (ii). error and complexity analysis, (2020), submitted, <https://hal.archives-ouvertes.fr/hal-02909750>.
 - [9] Patrick Joly, Maryna Kachanovska, and Adrien Semin, Wave propagation in fractal trees. Mathematical and numerical issues, *Netw. Heterog. Media* **14** (2019), no. 2, 205–264.
 - [10] Patrick Joly and Adrien Semin, Construction and analysis of improved Kirchoff conditions for acoustic wave propagation in a junction of thin slots, *Paris-Sud Working Group on Modelling and Scientific Computing 2007–2008*, *ESAIM Proc.*, vol. 25, EDP Sci., Les Ulis, 2008, pp. 44–67.
 - [11] Joly, Patrick and Semin, Adrien, Construction and analysis of improved kirchoff conditions for acoustic wave propagation in a junction of thin slots, *ESAIM: Proc.* **25** (2008), 44–67.
 - [12] C. Lubich, Convolution quadrature and discretized operational calculus. I, *Numer. Math.* **52** (1988), no. 2, 129–145.
 - [13] ———, Convolution quadrature and discretized operational calculus. II, *Numer. Math.* **52** (1988), no. 4, 413–425.
 - [14] Christian Lubich, Convolution quadrature revisited, *BIT* **44** (2004), no. 3, 503–514.
 - [15] Bertrand Maury, The respiratory system in equations, Springer-Verlag, 2013.
 - [16] Bertrand Maury, Delphine Salort, and Christine Vannier, Trace theorems for trees, application to the human lungs, *Network and Heterogeneous Media* **4** (2009), no. 3, 469 – 500.
 - [17] T. J. Royston, X. Zhang, H. A. Mansy, and R. H. Sandler, Modeling sound transmission through the pulmonary system and chest with application to diagnosis of a collapsed lung, *The Journal of the Acoustical Society of America* **111** (2002), no. 4, 1931–1946.
 - [18] Adrien Semin, Propagation d’ondes dans des jonctions de fentes minces, Ph.D. thesis, 2010.
 - [19] Lloyd N. Trefethen, Approximation theory and approximation practice, Society for Industrial and Applied Mathematics (SIAM), Philadelphia, PA, 2013.
 - [20] Ewald. R. Weibel, Morphometry of the human lung, Springer-Verlag, 1963.